APPENDIX A

METEOROLOGICAL MODELING FOR THE DFW ATTAINMENT DEMONSTRATION SIP FOR THE 2008 EIGHT-HOUR OZONE STANDARD

2015-014-SIP-NR

Proposal
December 9, 2015

APPENDIX A: METEOROLOGICAL MODELING FOR THE DFW ATTAINMENT DEMONSTRATION SIP FOR THE 2008 EIGHT-HOUR OZONE STANDARD

1. WEATHER RESEARCH AND FORECASTING (WRF) MODELING OVERVIEW

The Texas Commission on Environmental Quality (TCEQ) is using the WRF model version 3.2 to generate the meteorological inputs for the photochemical modeling supporting this State Implementation Plan (SIP) revision. The WRF modeling system was developed by a broad user community including the Air Force Weather Agency, national laboratories, and academia. Previous TCEQ SIP modeling used the Fifth Generation Meteorological Model (MM5) developed jointly by the NCAR and the Pennsylvania State University (PSU). The TCEQ has upgraded to the WRF model for two reasons; first, MM5 is no longer supported or maintained, and secondly, all new model improvements and developments are now incorporated into WRF. WRF modeling was conducted for the two time period listed in Table 1-1: DFW Meteorological Episodes.

Table 1-1: DFW Meteorological Episodes

Episode	All Grids Begin Date/Time (UTC)	All Grids End Date/Time (UTC)
June 2006	June 1, 2006 00:00	June 30, 2006 00:00
August 15 – September 15, 2006	August 15, 2006 00:00	August, 15, 2006 00:00

A Lambert Conformal Conic (LCC) map projection with geographical coordinates defined in Table 1-2: Lambert Conformal Map Projections was used for the WRF modeling.

Table 1-2: Lambert Conformal Map Projections

First True Latitude (Alpha):	33°N
Second True Latitude (Beta):	45°N
Central Longitude (Gamma):	97°W
Projection Origin:	97°W, 40°N
Spheroid:	Perfect Sphere, Radius = 6370 km

WRF was configured with two outer domains (36 km and 12 km horizontal grid resolution) with two-way nesting that cover the United States (U.S.) and south central portion of the country. A 4 km fine grid domain covering the eastern half of Texas is created with a one-way nesting to focus on metropolitan areas with air quality degradation. Figure 1-1: WRF Modeling Domains shows the WRF nested domain configuration. Each WRF grid embeds a corresponding CAMx grid of the same horizontal resolution. The easting and northing ranges for each grid in the LCC projection are defined in Table 1-3: WRF Modeling Domain Definitions in units of kilometers.

Vertically, WRF is defined by 43 layers from the surface to approximately 20 km as shown in Table 1-4: Vertical Layer Structure and presented graphically in Figure 1-2: WRF Vertical Layer Structure on a sigma coordinate system. 20 layers are within the first 3000 meters in order to resolve boundary layer phenomena and to provide a one-to-one mapping with the first 20 layers for CAMx. The same WRF vertical layering structure is used for all of the domains.

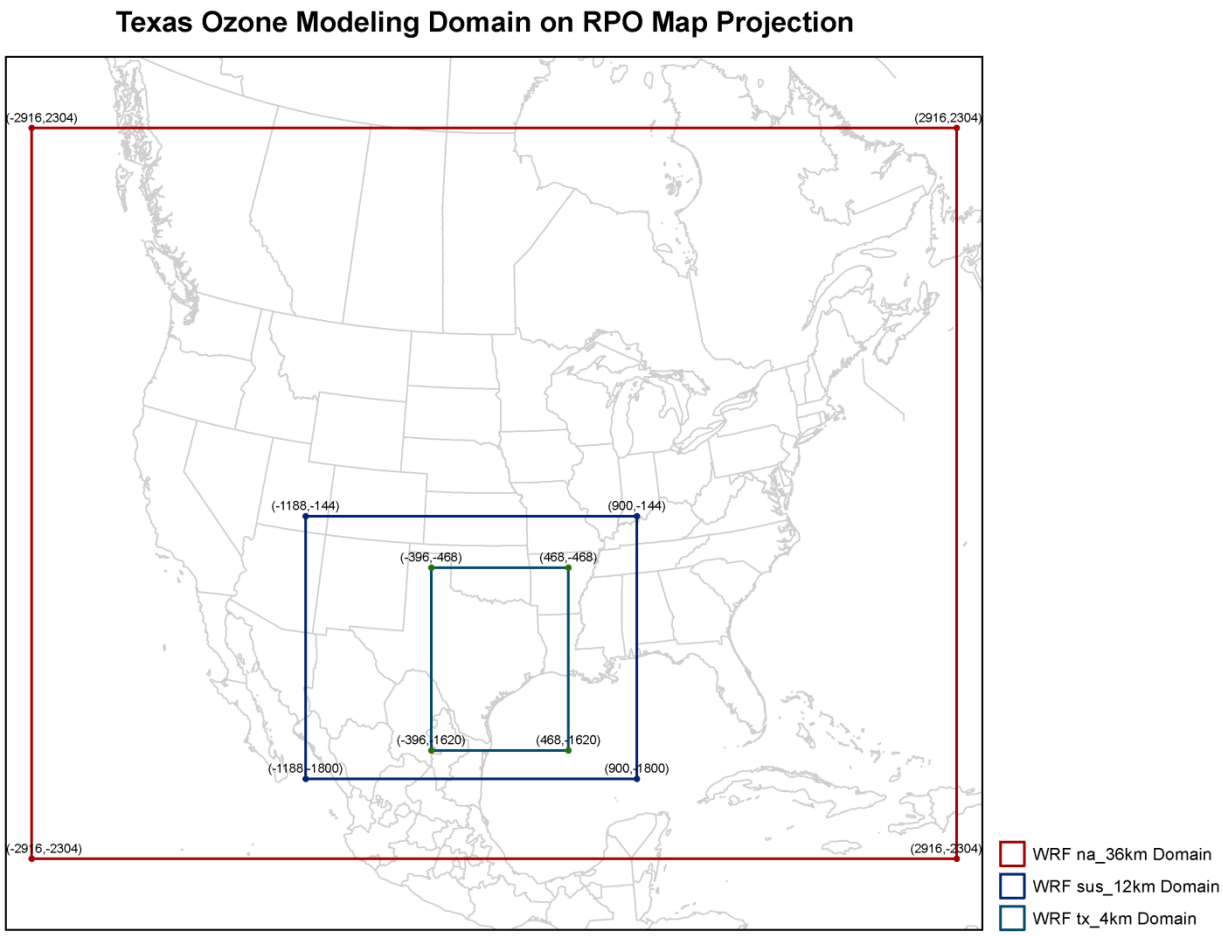

Figure 1-1: WRF Modeling Domains

Table 1-3: WRF Modeling Domain Definitions

Domain	Easting Range (km)	Northing Range (km)	East/West Grid Points	North/South Grid Points
36 km	(-2916,2916)	(-2304,2304)	163	129
12 km	-1188,900)	(-1800,-144)	175	139
4 km	(-396,468)	(-1620,-468)	217	289

Table 1-4: Vertical Layer Structure

Layer	Sigma	Layer Top (m AGL)	Center (m AGL)	Thickness (m)
43	0.000	20806.8	20362.1	889.6
42	0.010	19917.3	19341.4	1151.7
41	0.025	18765.6	18117.9	1295.3
40	0.045	17470.3	16918.8	1103.1
39	0.065	16367.2	15773.2	1188.1
38	0.090	15179.1	14662.7	1032.8
37	0.115	14146.3	13602.4	1087.8
36	0.145	13058.5	12577.6	961.9
35	0.175	12096.6	11596.6	1000.0
34	0.210	11096.7	10587.9	1017.5
33	0.250	10079.1	9622.9	912.6
32	0.290	9166.6	8752.3	828.6
31	0.330	8338.0	7958.1	759.8
30	0.370	7578.2	7269.5	617.3
29	0.405	6960.9	6671.3	579.2
28	0.440	6381.7	6108.8	545.8
27	0.475	5835.9	5577.7	516.3
26	0.510	5319.5	5108.7	421.6
25	0.540	4898.0	4695.9	404.0
24	0.570	4493.9	4299.9	388.0
23	0.600	4105.9	3919.3	373.3
22	0.630	3732.7	3552.8	359.7
21	0.660	3373.0	3199.5	347.1
20	0.690	3025.9	2858.2	335.5
19	0.720	2690.4	2528.1	324.6
18	0.750	2365.8	2234.4	262.8
17	0.775	2103.0	1974.9	256.1
16	0.800	1846.9	1721.9	249.8
15	0.825	1597.0	1475.1	243.9
14	0.850	1353.2	1281.4	143.6
13	0.865	1209.6	1138.8	141.6
12	0.880	1068.0	998.1	139.7
11	0.895	928.3	859.4	137.8
10	0.910	790.5	745.0	90.9
9	0.920	699.6	654.6	90.1
8	0.930	609.5	564.9	89.3
7	0.940	520.2	476.0	88.5
6	0.950	431.7	387.8	87.8
5	0.960	343.9	300.4	87.0
4	0.970	256.9	213.7	86.3
3	0.980	170.5	127.7	85.6
2	0.990	84.9	59.4	51.0
1	0.996	33.9	16.9	33.9
0	1.000	0.0	0.0	0.0

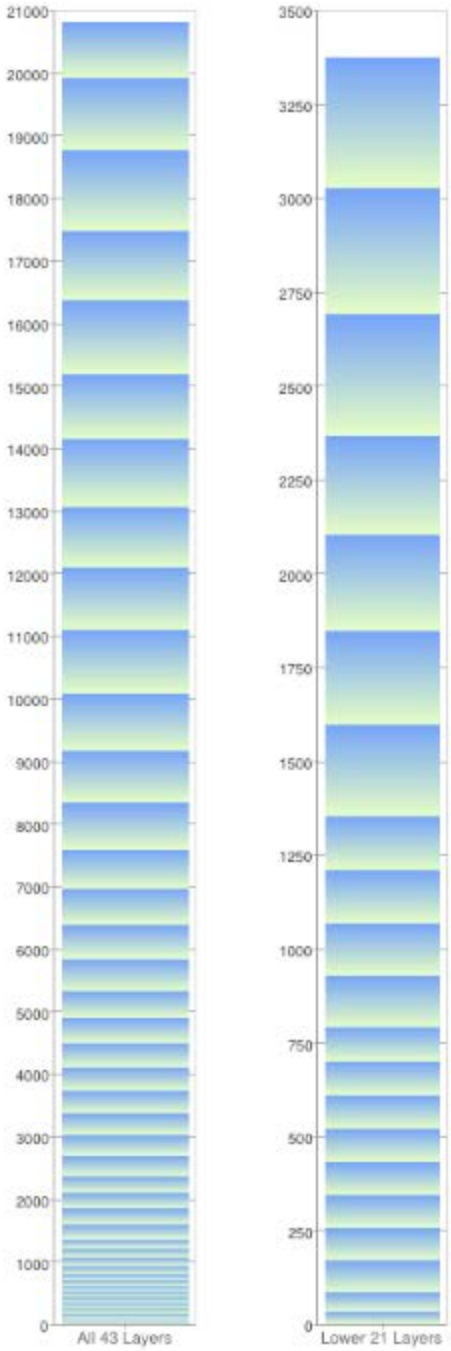

Figure 1-2: WRF Vertical Layer Structure

2. WRF CONFIGURATION

The final meteorological modeling configuration for the two episodes during 2006 was the result of numerous sensitivity tests and model performance evaluation. The preparation of WRF input files involves the execution of different models within the WRF Preprocessing System (WPS). Analysis nudging files are generated as part of WPS preparation of WRF input and boundary

condition files. Observational nudging files with radar profiler data were developed in-house by agency staff outside of the WPS System.

GEOGRID

- Defines the WRF grids on a Lambert-Conformal Projection (see Table A-2 above).
- New Land Use/Land Cover (LULC) data overwrite of default USGS data for east Texas.

UNGRIB/METGRID

- Unpacking of GRIB files with surface and upper level meteorological data on a user-defined sub-set of standard pressure level data as well as Sea Surface Temperature (SST) data.

- Re-gridding the unpacked data onto the WRF grids defined in Geogrid in a NetCDF format.

REAL

- Base state variables were set to Texas summer values: 1013 hPa sea-level pressure, a reference temperature lapse rate of 45 (K/ln p), and a 304 °K sea-level temperature

It is beyond the scope of this SIP Appendix to document all WRF configurations tested as part the June 2006 performance evaluation. However, the following points are of particular importance for the purposes of producing meteorology for photochemical modeling. First, low level wind speed and direction are given greater importance that surface (2 meter) temperature. For air quality applications, the strength and depth of the planetary boundary layer are considered important; however, without the availability to directly measure this feature, lower tropospheric winds as measured by the nearest domain radar profiler is important. Also of critical importance is cloud coverage.

The TCEQ continued this work on the June 2006 episode by contract with Environ, which resulted in an MM5 configuration that yielded good performance in the DFW and central Texas areas (Emery et al., 2009b). Observational nudging using TexAQS II radar profiler data and one-hour surface analysis nudging improved wind performance. Switching from the NOAH (NCEP Oregon State Air Force Hydrological Research Laboratory) Land-Surface Model to the five-layer soil model also improved the representation of precipitation, temperature, and planetary boundary layer (PBL) depths.

The TCEQ continued to improve upon the performance of WRF for the June 2006 episode through a series of sensitivities. The final WRF parameterization schemes and options selected are shown in Table 2-1: June 2006 WRF Configuration. The selection of these schemes and options was based on extensive testing of model configurations that were intended to build upon previous experience with MM5 modeling in previous SIP demonstrations. Among all the meteorological variables that can be validated, minimizing wind speed bias was the highest priority for model performance consideration.

Table 2-1: June 2006 WRF Configuration

Domain	Nudging Type	PBL	Cumulus	Radiation	Land-Surface	Microphysics

Domain	Nudging Type	PBL	Cumulus	Radiation	Land-Surface	Microphysics
36 km and 12 km	3-D, Surface Analysis, & Obs	YSU	Kain-Fritsch	RRTM / Dudhia	5-layer soil model	WSM6
4 km	3-D, Surface Analysis, & Obs	YSU	None	RRTM / Dudhia	5-layer soil model	WSM6

Note: RRTM = Rapid Radiative Transfer Model

WRF output was post-processed using the WRFCAMX version 6.3 utility to convert the WRF meteorological fields to the Comprehensive Air Quality Model with Extensions (CAMx) grid and input format (Environ, 2010). The WRFCAMX now generates several alternative vertical diffusivity (K_V) files based upon multiple methodologies for estimating mixing given the same WRF meteorological fields. The Kv option to match WRF YSU PBL has been used for the CAMx runs described in this document.

3. WRF MODEL PERFORMANCE EVALUATION (MPE) TOOLS

3.1 Observations

To evaluate the performance of WRF, comparisons to observed data are made. For surface data, the TCEQ Continuous Air Monitoring Stations (CAMS) are used for comparison. There were over 100 CAMS in the WRF 4 km domain and 25 in the DFW Region 4 Figure 3-1: All WRF 4km TCEQ CAMS (left) and DFW Region 4 CAMS (right) during the 2006 modeling period. Because of the large number of CAMS monitors in the DFW region, an area wide average may smooth out smaller scale features. Eight monitors throughout the DFW area were chosen to represent smaller geographic areas as defined in Figure 3-2: Selected DFW CAMS for MPE. Evaluating model runs using the DFW Region area and a subset of individual monitors instead of all CAMS monitors proved to be efficient, allowing for the evaluation of more modeling sensitivities.

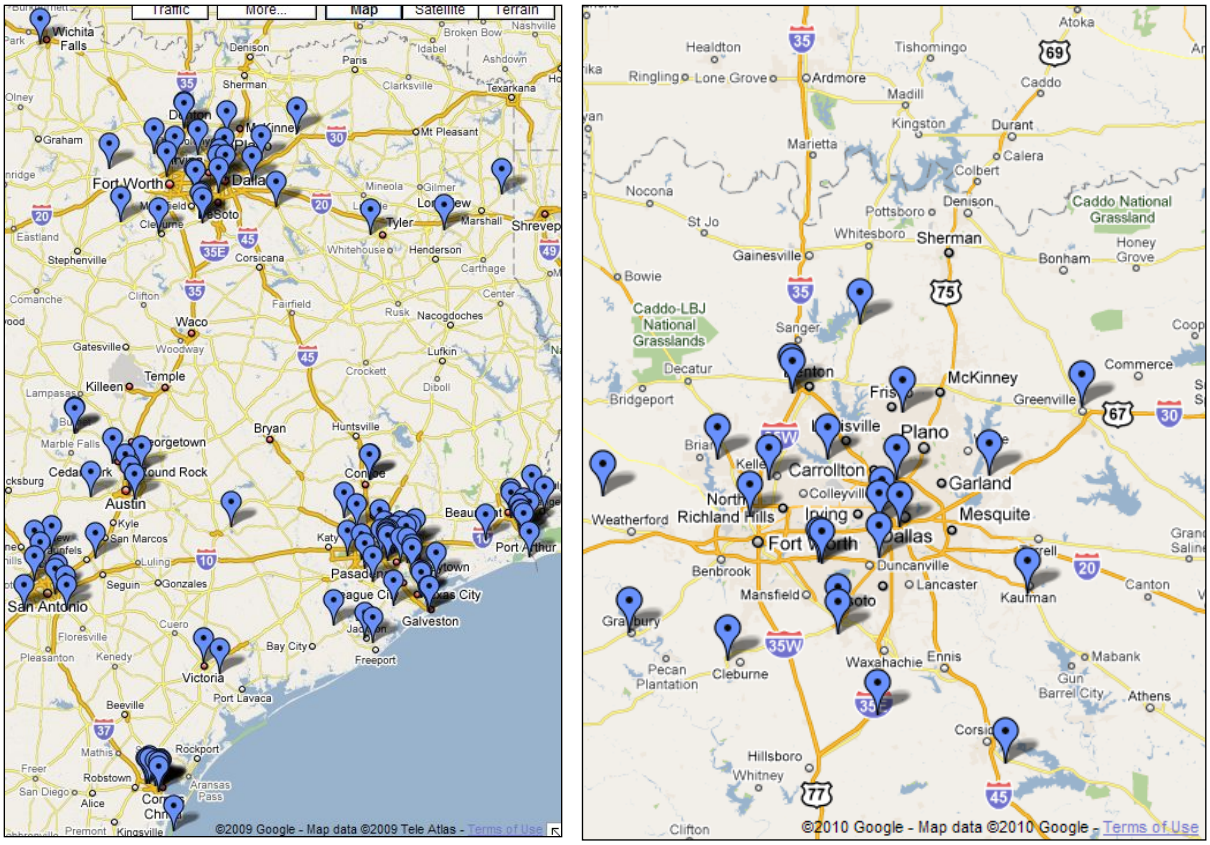

Figure 3-1: All WRF 4km TCEQ CAMS (left) and DFW Region 4 CAMS (right)

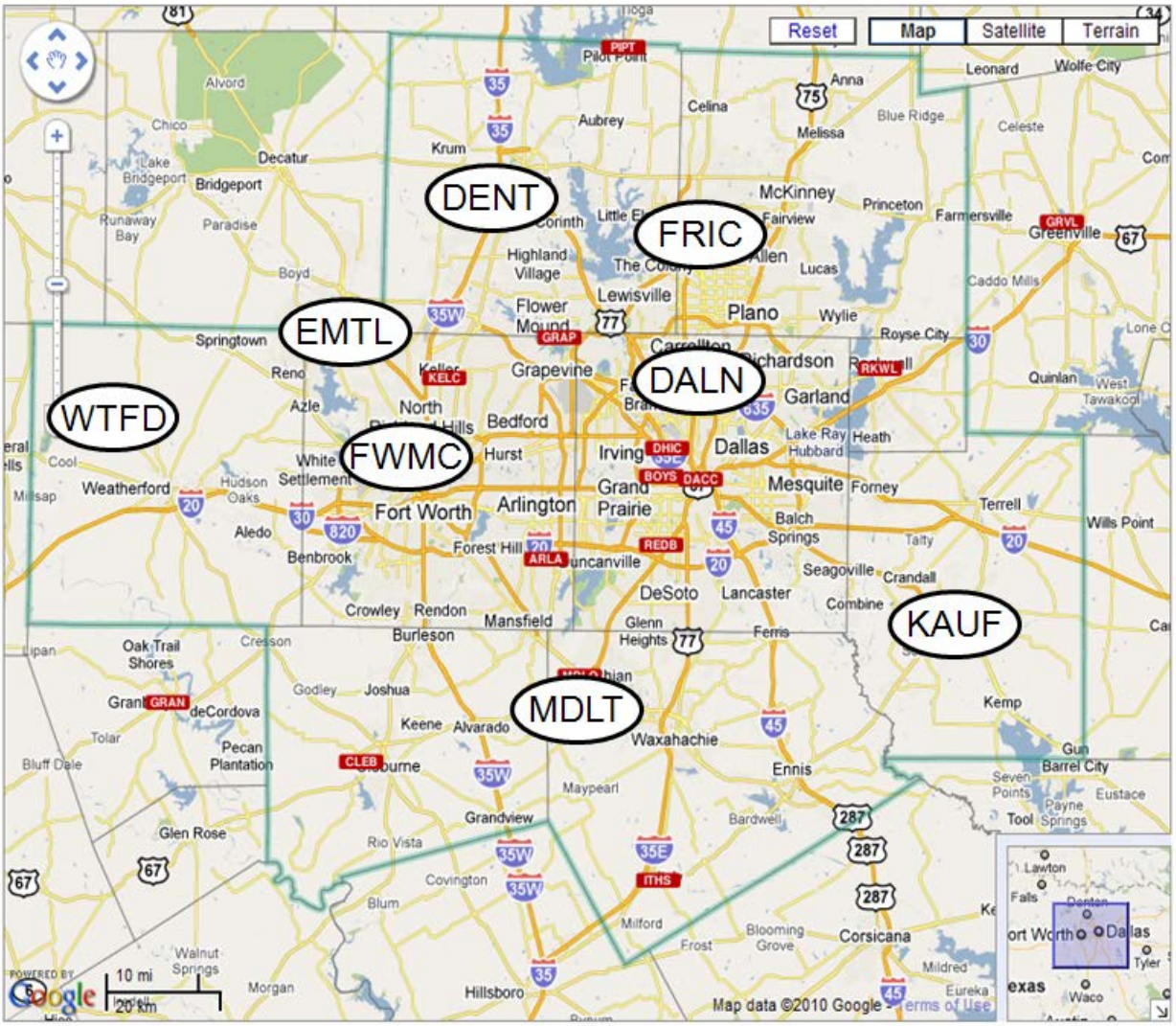

Figure 3-2: Selected DFW CAMS for MPE

The TexAQS II profiler network was used to evaluate the performance of WRF winds above the surface layer. Up to 15 profilers collected data during the 2006 modeling, including estimates of PBL depth. Profiler locations are shown below in Figure 3-3.

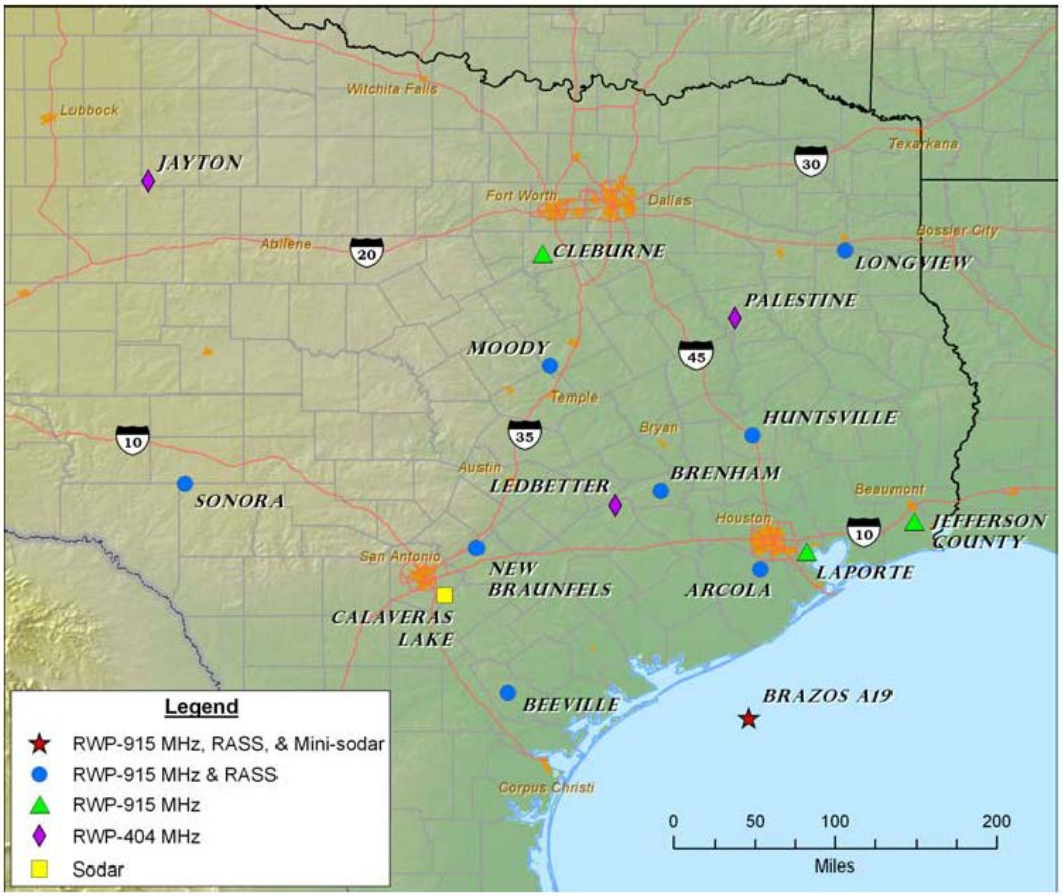

Figure 3-3: Profilers in 4km WRF domain

3.2 Time Series Panel

Time series panels comparing modeled and observed CAMS surface wind direction, wind speed, and temperature were created to evaluate the model's performance over the entire episode. The observations are hourly averages of individual and grouped monitors (e.g. TCEQ Region-wide, or domain-wide). As an example of a time series panel Figure 3-4: Dallas Executive Airport C402 wind speed time series, shows the time series of hourly wind speed for the Dallas Executive Airport. The X axis of the time series panels is the date and time in Central Standard Time (CST) of the modeling episode. The Y axis represents the range of values of the parameter (e.g. wind speed). The title of the panel indicates the geographic region, parameter (wind speed, temperature, etc.), model and run name.

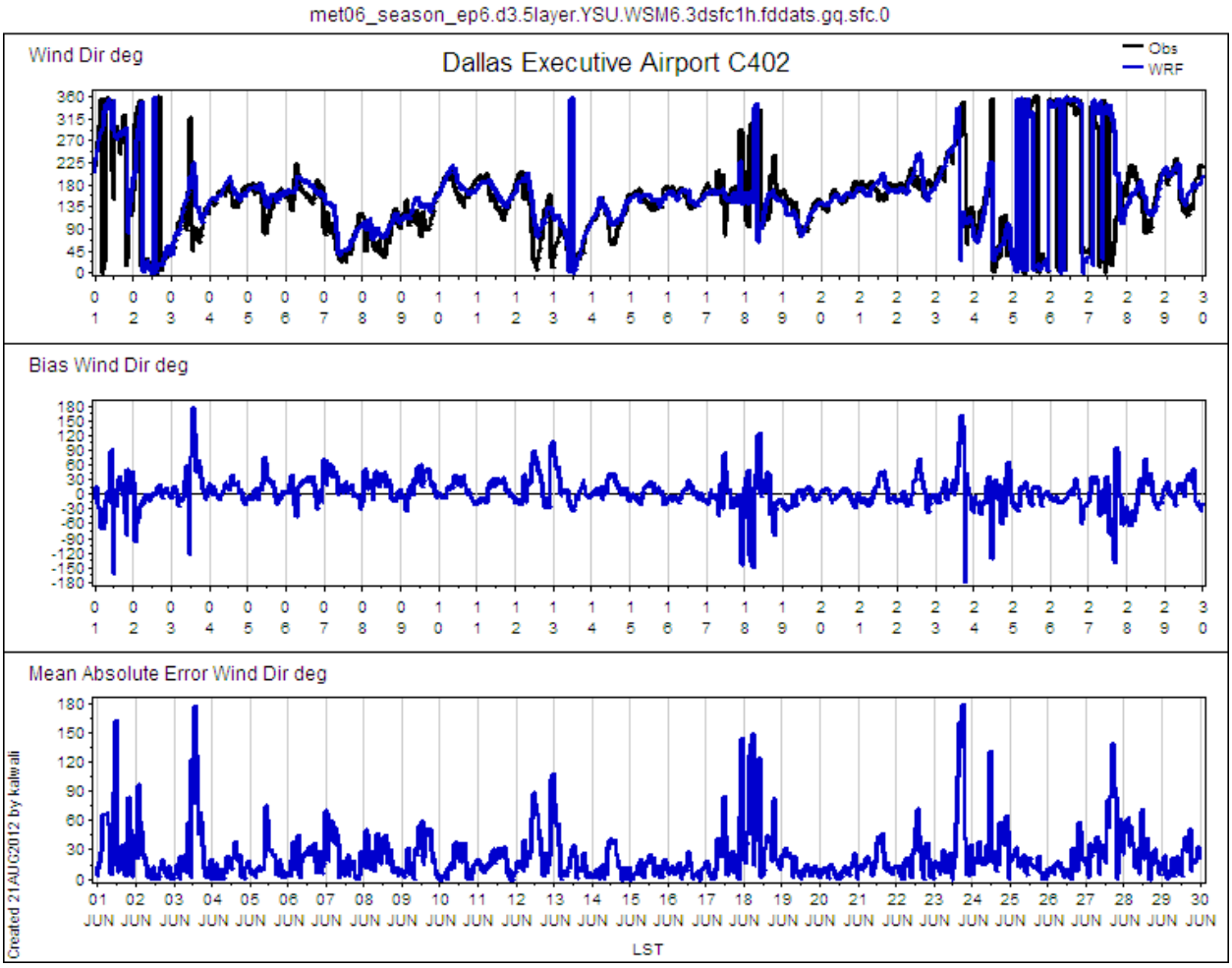

Figure 3-4: Dallas Executive Airport C402 wind speed time series

3.3 Scatter Plots

Scatter plots of model versus observations were created to correlate how well the model statistically performs at monitors (groups of monitors), episode days, and model layers. As with the time series, the model is compared to individual, region-wide, and domain-wide groups of monitors for every hour (per day or episode). For surface data, the observations are compared to the model's first layer values. The percent of hours (all, day, or night) where the model is within the accuracy benchmarks (e.g. wind direction less than or equal to 30 degrees or wind speed less than or equal to 2 meters per second) is depicted in the upper right of the plot. Tables of these accuracy percentages are also presented to summarize the scatter plots.

A linear regression line is fitted to the data and is shown in green. The correlation equation and coefficient of determination R^2 for the regression line is above the plot in green. For the model to perfectly fit the data the regression line would fall on the one-to-one line and the R^2 would be 1.0. The R^2 indicates how well WRF predicts the observations, with higher values indicating better model performance. As the model is an imperfect representation of the real world and the observations have biases, errors, and limitations, a perfect fit is not expected. In fact a perfect fit (or very close to it) may be reason to suspect that WRF is being nudged too hard (see Attachment 3: Data Assimilation). For wind direction, the regression line and R^2 are not calculated since both 0° and 360° symbolize north winds and make those statistics meaningless.

The plot titles are the same as the time series. For the scatter plots, the X axis is the observed data and the Y axis is the modeled. The total number of date-time points (hours) and observations (hour-monitor pairs) that comprise the plot are listed next to the parameter name. Figure 3-5: Keller C17 wind speed scatter plot shows an example of Keller C17's wind speed over the June 2006 episode.

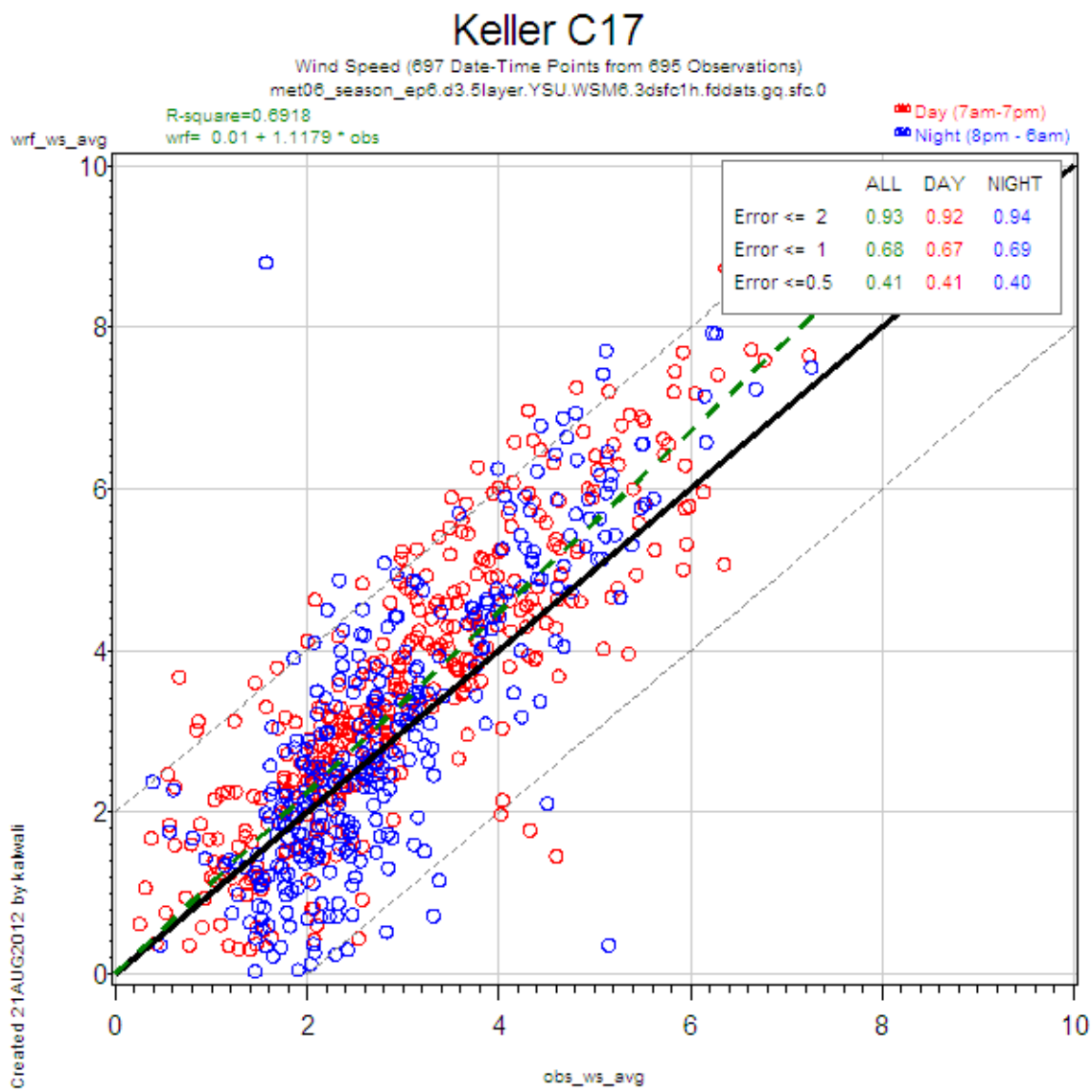

Figure 3-5: Keller C17 wind speed scatter plot

3.4 WRFCAMx Cloud Optical Depth and GOES Cloud Fraction

Early ozone pollution meteorology ignored clouds since episodes were short and selected for clear conditions or during periods of high pressure subsidence associated with ozone production. However, as air quality episodes have become longer in length, due in part to lower ozone standards, the importance of properly capturing cloud coverage becomes increasingly important. First this because longer episodes will include cloudy weather, and secondly, cloud prediction is important because subtle differences strongly impact daily ozone values.

Cloud optical depth is a parameter that is used in the photochemical model to modify photolysis rates in chemical reactions. This meteorological parameter is not directly output from WRF but calculated in the post-processing program WRFCAMx which prepares WRF output for CAMx modeling. Cloud fraction, as captured in the visible bands of Geostationary Orbiting Environmental Satellite (GOES) data, is a surrogate for proper cloud placement and approximates the amount of solar radiation available to participate in chemical reactions. Throughout both June 2006 and August and September 2006, WRF cloud prediction, as represented by the cloud optical depth calculated for the CAMx model, compared very favorably to GOES data. One example of the correspondence between the calculated cumulative cloud optical depth output from WRFCAMx and the GOES observed cloud fraction is in Figure 3-6: June 4, 2006: WRFCAMx Cloud Optical Depth and GOES Cloud Fraction.

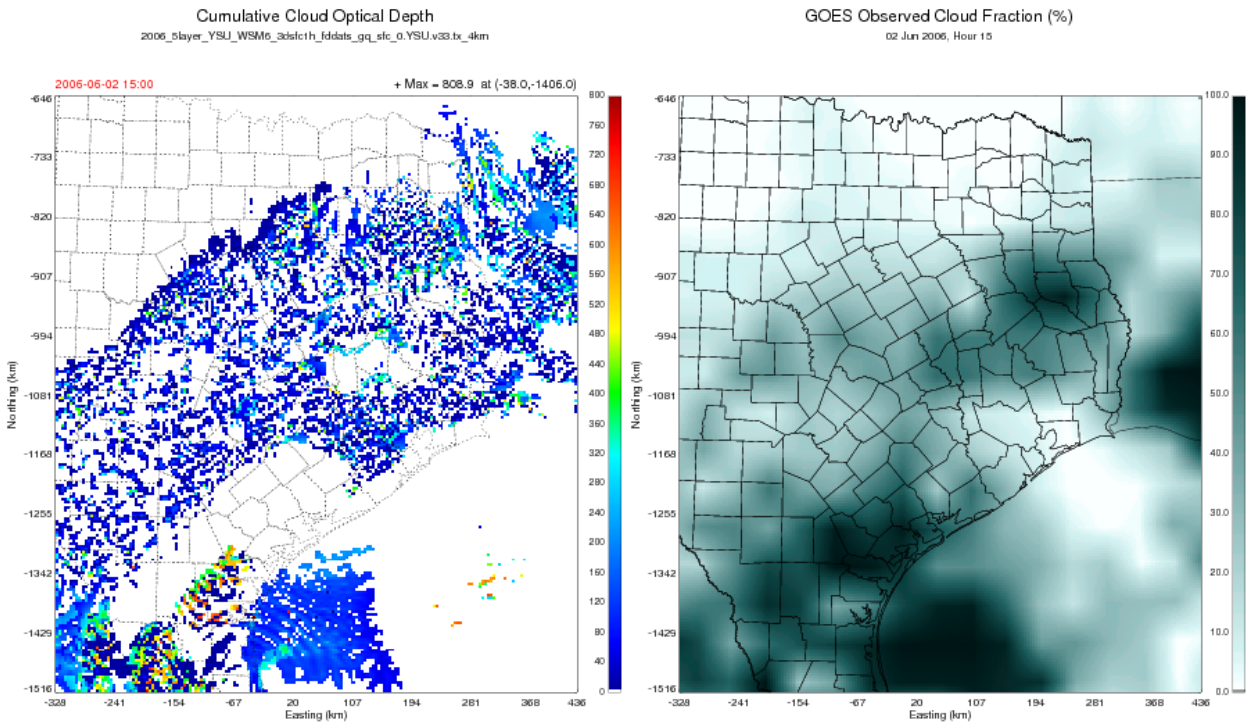

Figure 3-6: June 4, 2006: WRFCAMx Cloud Optical Depth and GOES Cloud Fraction

3.5 Time-height plots

Time-height plots represent the upper air horizontal wind conditions at profiler locations over one episode day. Vertical winds (rising or descending air) are not shown. The model winds (CAMx input) are shown as blue vectors and the observed winds (profiler) are shown as red vectors. Each hour of the episode day is depicted on the x-axis. Winds from just above the surface to 3 km are illustrated by vectors pointing in the compass direction from where the wind is blowing. A longer vector indicates faster wind speeds. The Cleburne profiler is the only profiler within the 4 km CAMx domain for DFW. In Figure 3-7: Time-height plot example (6/2/2006 at Cleburne profiler) below, at 4 AM CST on 6/2/2006 a southwest wind greater than 10 m/s blows at 2.5 km above the surface at the Cleburne profiler (red vector). The model predicts more southerly winds and lighter (blue vector). Observed winds were not available midnight to 3 AM and 11 PM on this day.

Also on these plots are the model (blue) and profiler (red) estimated PBL depths shown by horizontal lines between hours. The observed data is generally only available during daylight hours. At 4 PM CST in Figure 3-7 below, the model and observed PBL depth agree well but differ by 800 meters at 5 PM.

Based on Knoderer et al. (2008), the morning rise of the PBL may be more important to ozone production than the peak mixing depth. The morning rise was focused on for model performance evaluation as well as gross differences. More information regarding the derivation of mixing heights from the radar wind profiler data can be found in Knoderer and MacDonald (2007).

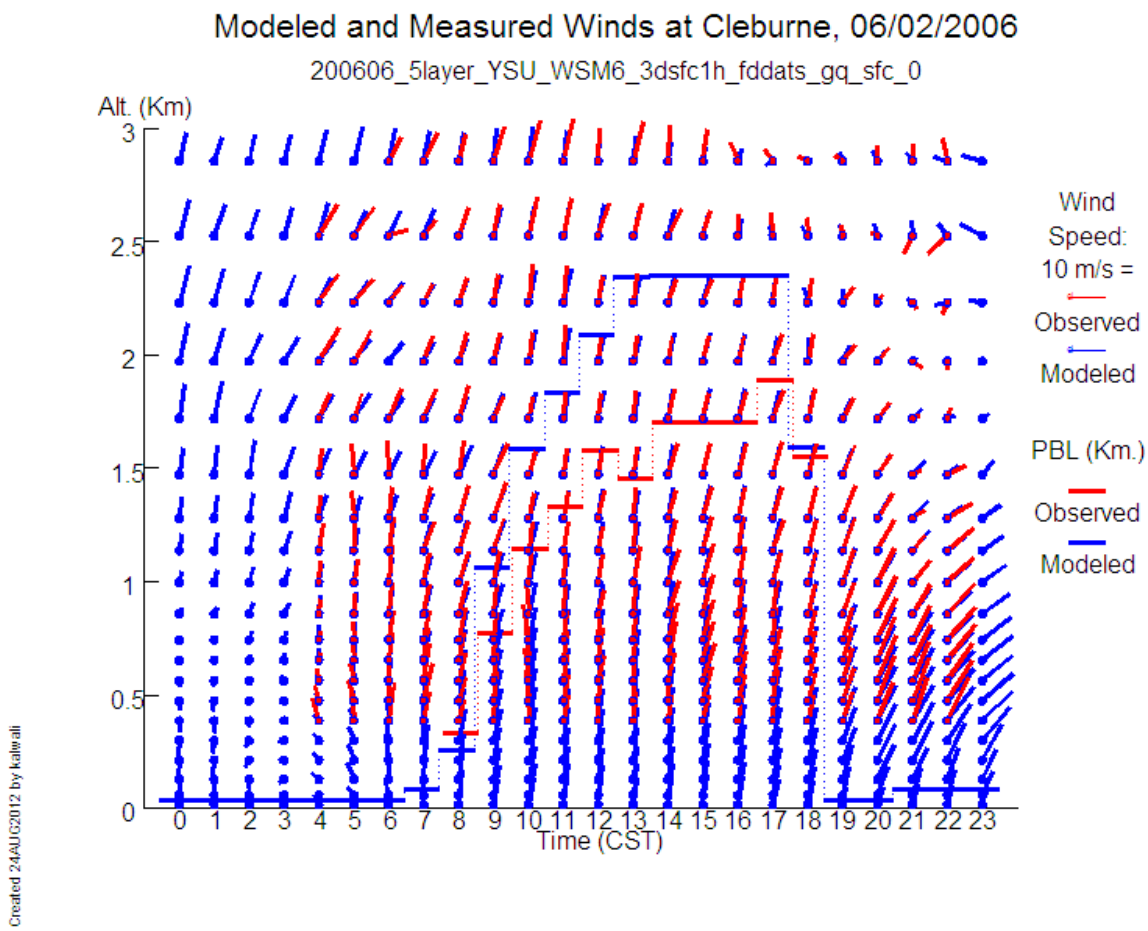

Figure 3-7: Time-height plot example (6/2/2006 at Cleburne profiler)

4. WRF MODELING PERFORMANCE

The following sections describes the performance of the final WRF modeling configuration for the June 2006 episode and August-September 2006 episode. Due to the large number of episode days, the performance evaluation will focus on the days when high ozone and notable meteorological phenomena occurred (Knoderer et al., 2008; Nielsen-Gammon, 2007a; Nielsen-Gammon, 2007b; TCEQ, 2006). Wind field performance was deemed to be the most important for photochemical modeling input followed by temperature, PBL height, and other important features.

4.1 June 2006 Episode Performance Evaluation

The June 2006 episode had seventeen days (out of 30) with an observed eight-hour ozone exceedance. Sixteen of those days had more than five DFW monitors exceeding 75 ppb. The two highest eight-hour ozone exceedances of 2006 also occurred during this episode.

As noted in the DFW Modeling Protocol and Conceptual Model, the June 2006 episode experienced meteorological conditions similar to typical ozone exceedance days. Slow east, southeast, and south winds were observed as were clear skies with high temperatures on many days. Several frontal passages also swept through DFW, which have shown to bring stagnant conditions favorable for ozone formation (McNider, 2009).

The WRF modeling was evaluated by comparing the hourly modeled and measured wind speed, wind direction, and temperature for all monitors in the DFW area Figure 4-1: June 2006 Meteorological Modeling Performance exhibits the percent of hours for which the average absolute difference between the modeled and measured wind speed and direction, for specific monitors and a DFW area average, was within the specified accuracy benchmarks (e.g., wind speed difference less than or equal to two meters per second: WSPD ≤ 2 m/s). All performance evaluation products are available on TCEQ's ftp site: http://www.tceq.state.tx.us/airquality/airmod/

).

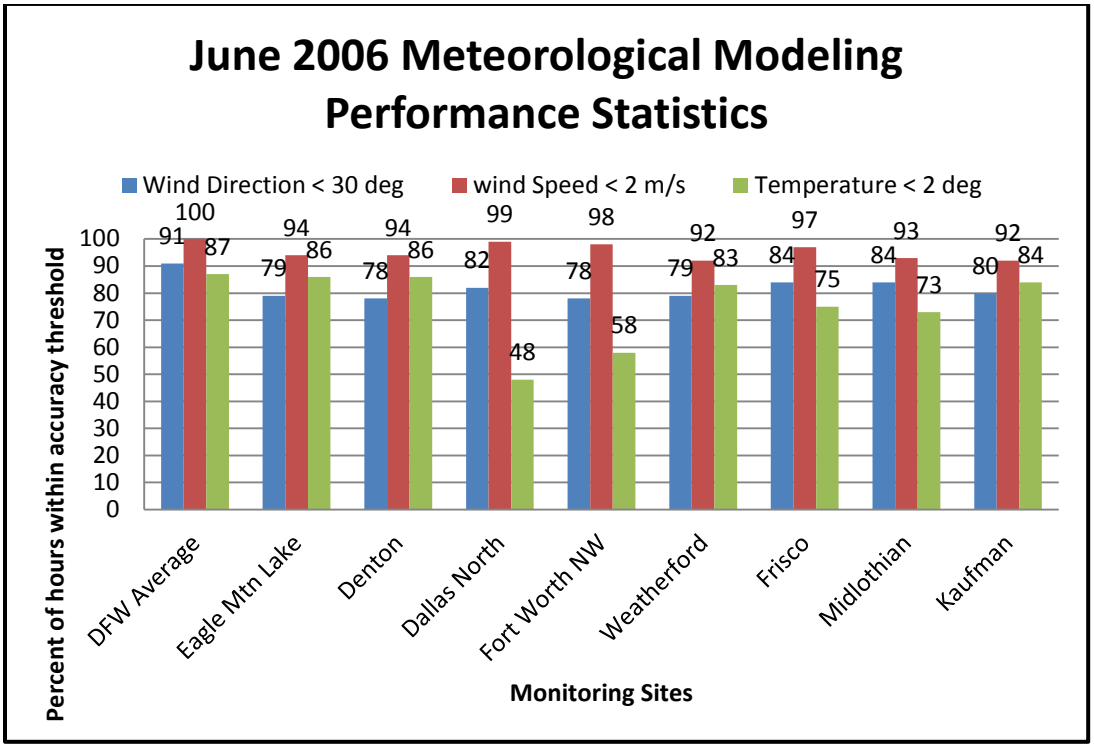

Notes: WDIR = Wind Direction; WSPD = Wind Speed; TEMP = Temperature

Figure 4-1: June 2006 Meteorological Modeling Performance

As Figure A-10 shows for the DFW area, WRF performed well for wind speed and direction reasonably well for temperature. As noted above, the WRF configuration was selected for optimal performance on low level wind speed since this meteorological variable so strongly

impacts CAMx performance. Wind speed performance was excellent at the individual monitors , but note that observed wind direction is less accurate when wind speeds are low, a condition often observed during ozone exceedances.

Table 4-1: DFW Meteorological Modeling Percent Accuracy provides an additional evaluation of WRF predictions to stricter benchmarks (Emery et al., 2001). The model's ability to replicate wind direction and speed within 20 degrees and 1 m/s on average enhances the confidence in this modeling setup.

Table 4-1: DFW Meteorological Modeling Percent Accuracy

DFW Area	Wind Direction (°) Error ≤ 30 / 20 / 10	Wind Speed (m/s) Error ≤ 2 / 1 / 0.5	Temperature (°C) Error ≤ 2 / 1 / 0.5
Area Average	91 / 83 / 65	100 / 89 / 64	87 / 39 / 14
Eagle Mountain Lake	79 / 69 / 48	94 / 68 / 40	86 /44 / 18
Denton	78 / 64 /35	94 / 64 / 32	86 / 66/ 45
Dallas North	82 / 71 / 42	99 / 83 / 51	48 / 23 / 08
Fort Worth NW	78 / 68 / 42	98 / 83 /54	58 / 20 / 08
Weatherford	79 / 67 / 42	92 / 66 / 37	83 / 44 / 20
Frisco	84 / 73 / 47	97 / 74 / 42	75 / 35 / 16
Midlothian Tower	84 / 72 / 45	93 / 70 / 41	73 / 41 / 24
Kaufman	80 / 68 / 43	92 / 67 / 34	84 / 46 / 25

Figure 4-2: DFW Area Average Wind Direction and Speed Scatter Plots present the model's prediction versus the observations for each hour of the episode for wind direction and speed. Night and daytime hours are depicted by blue and red circles, respectively. Very few hours (circles) fell outside the error benchmarks, indicating the model performed well on average.

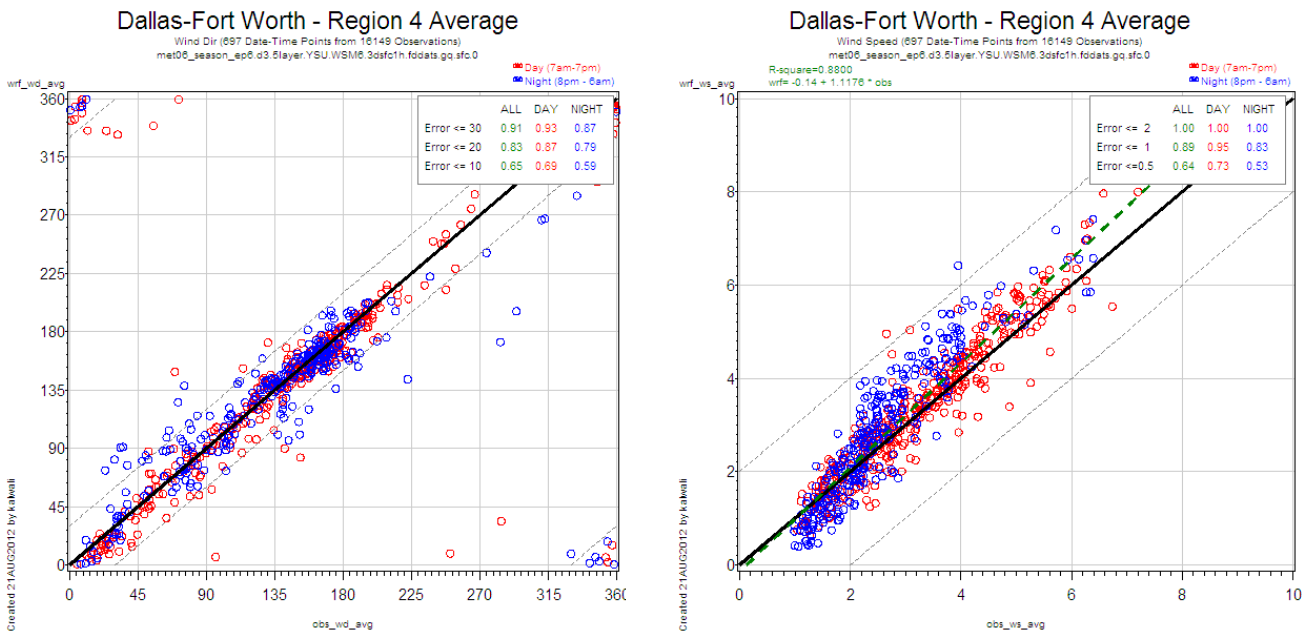

Figure 4-2: DFW Area Average Wind Direction and Speed Scatter Plots

The following three plots exhibit the wind direction, wind speed, and temperature time series of the average of all DFW monitors. WRF follows the observations closely for almost all time periods. The wind patterns near frontal passages appear to have the highest bias and error (e.g. June 1-2, June 13-14, June 18) as shown in Figure 4-3: DFW Average Wind Direction Time Series and Figure 4-4: DFW Average Wind Speed Time Series. On most days WRF closely matched diurnal temperature profiles Figure 4-5: DFW Average Temperature Time Series. One important note, though, is that the diurnal pattern in the temperature *bias* is attributed to the use of the five layer thermal diffusion scheme which does not model moisture as would a land surface model. However, as noted in the discussion above about this WRF configuration, the emphasis on wind speed and direction led to this model choice.

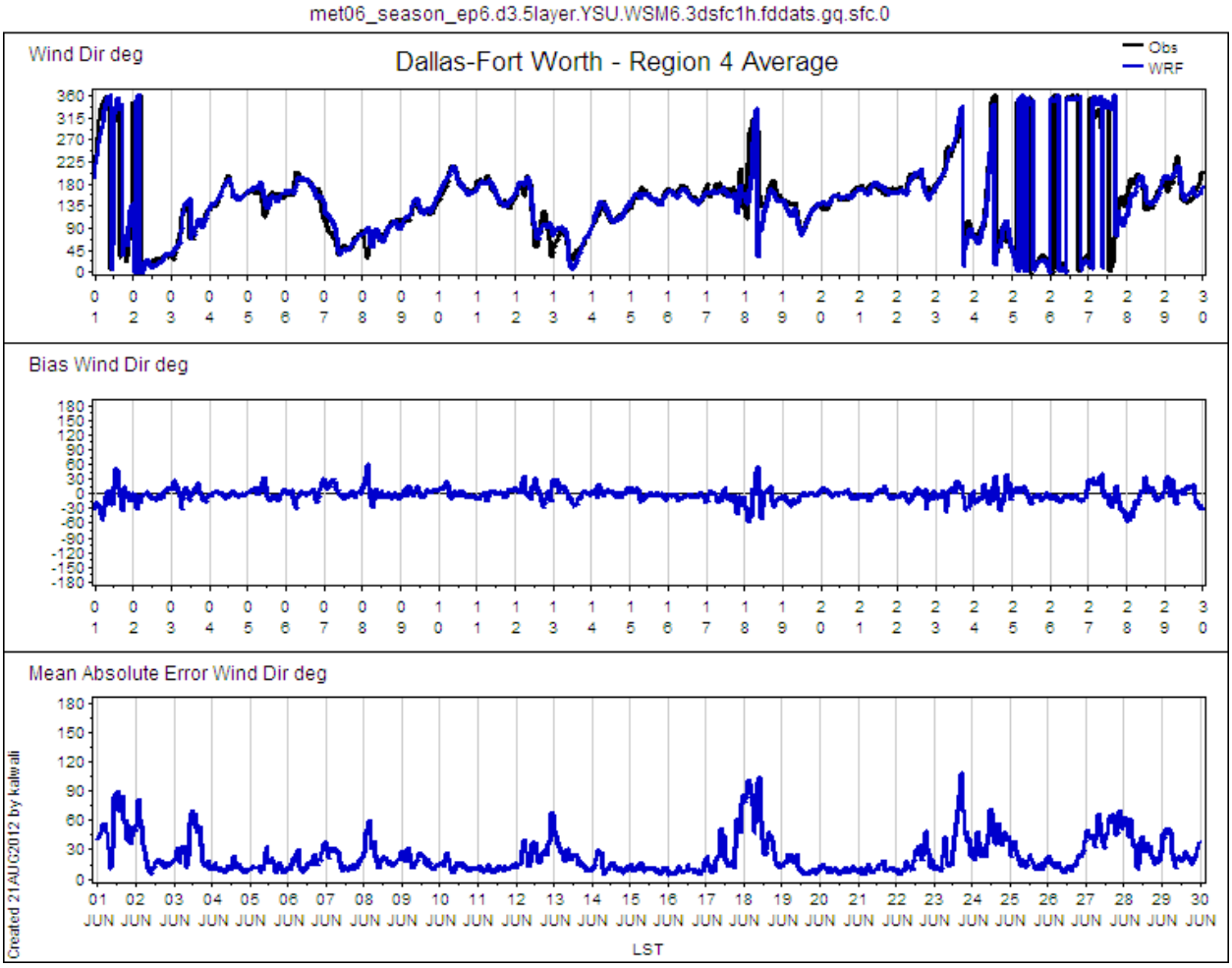

Figure 4-3: DFW Average Wind Direction Time Series

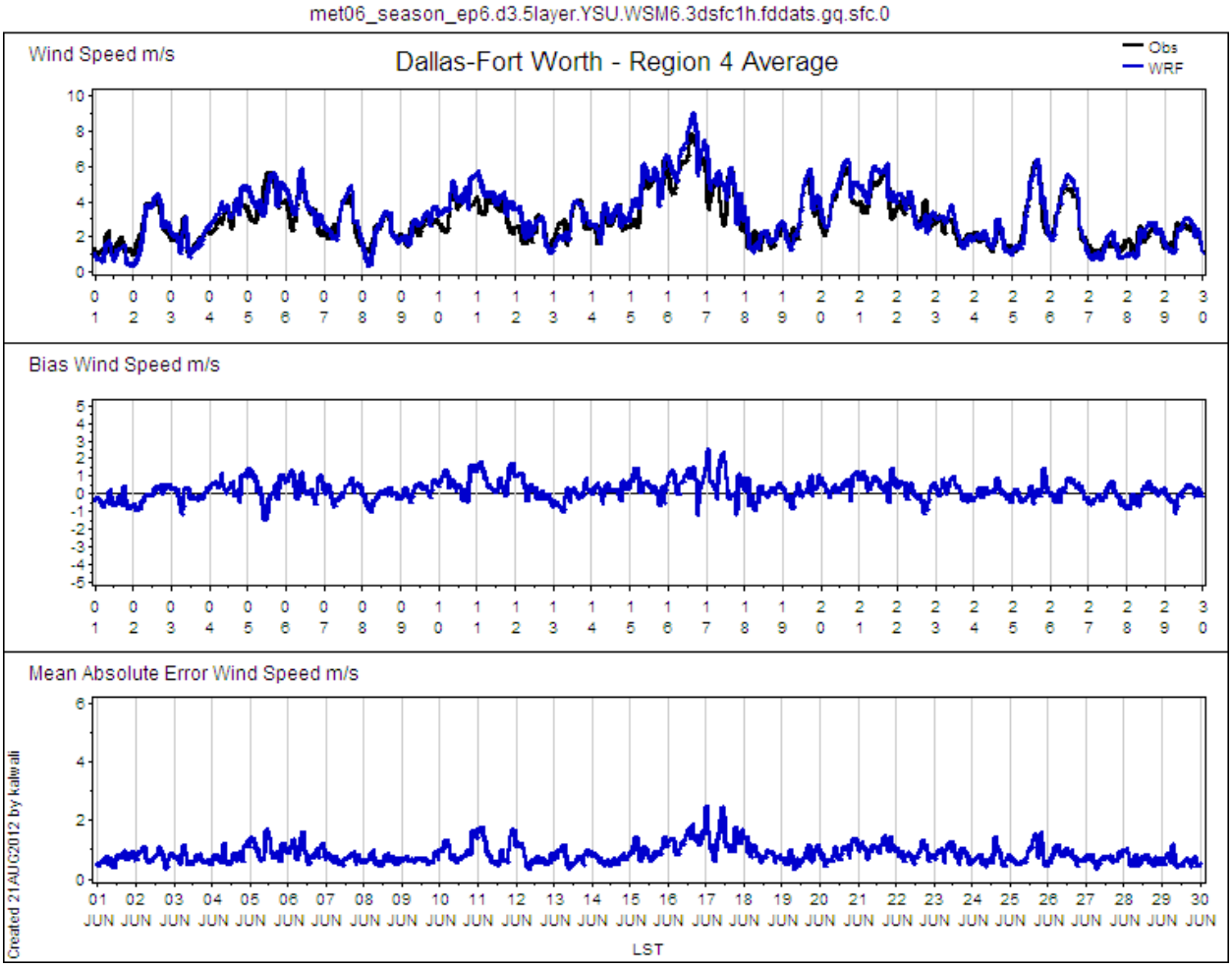

Figure 4-4: DFW Average Wind Speed Time Series

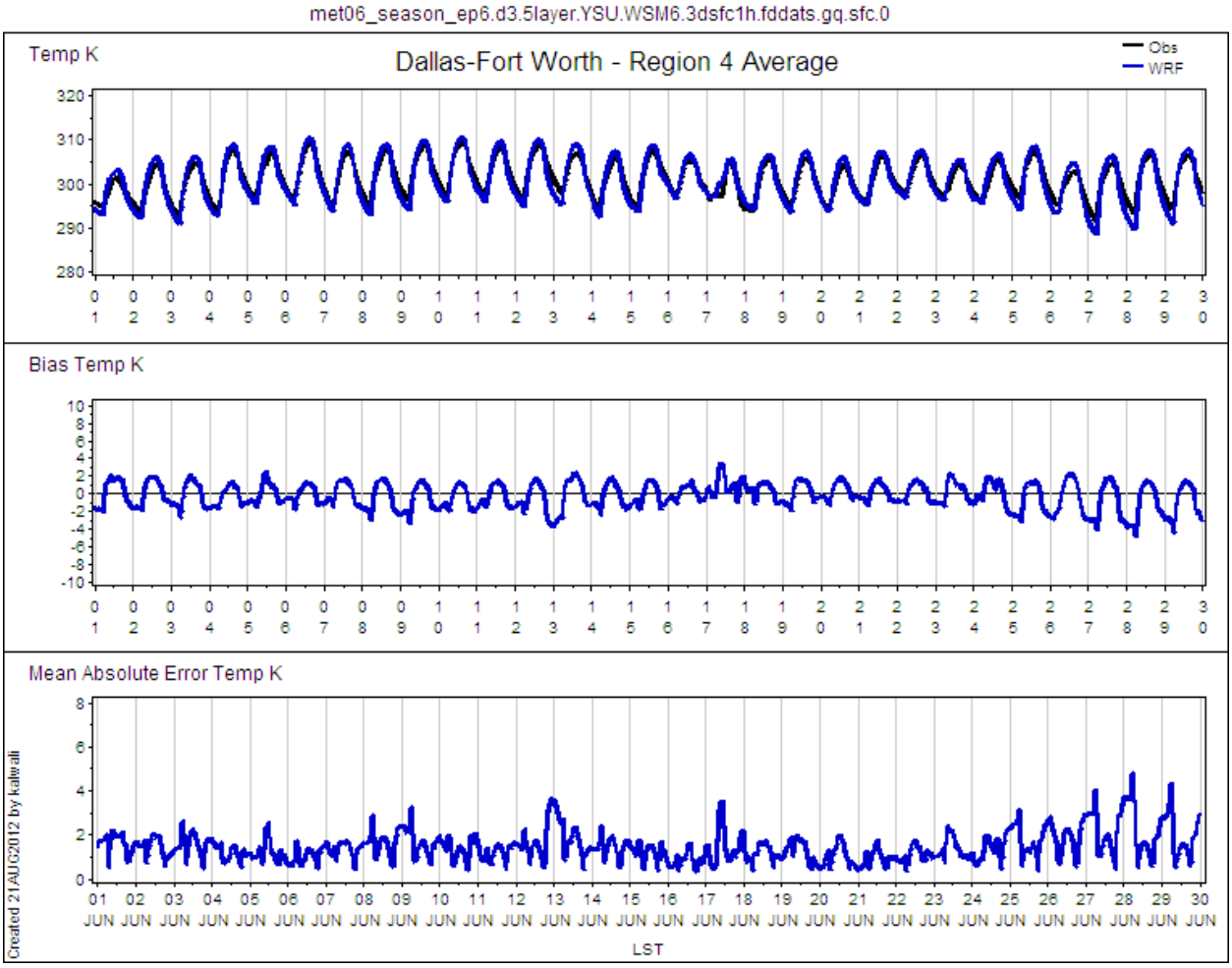

Figure 4-5: DFW Average Temperature Time Series

4.2 June 9, 2006 Performance Evaluation

Clear skies, high temperatures, and slow south-easterly winds contributed to the high ozone on June 9, 2006 as high pressure was centered over northern Louisiana and southern Arkansas. The peak eight-hour ozone was 106 ppb at Eagle Mountain Lake and Denton Airport. Eight monitors recorded eight-hour exceedances, all on the west and north sides of DFW. The winds were very stable on this day and the model replicated those conditions very well Figure 4-6: June 9, 2006 Wind Direction and Speed Scatter Plots. Table 4-2: June 9, 2006 Meteorological Modeling Percent Accuracy shows that the wind direction and wind speed accuracy was good even for higher thresholds for accuracy. Temperature performance was also good.

Table 4-2: June 9, 2006 Meteorological Modeling Percent Accuracy

DFW Area	Wind Direction (°) Error ≤ 30 / 20 / 10	Wind Speed (m/s) Error ≤ 2 / 1 / 0.5	Temperature (°C) Error ≤ 2 / 1 / 0.5
Area Average	100 / 100 / 88	100 / 100 / 75	71 / 25 / 08

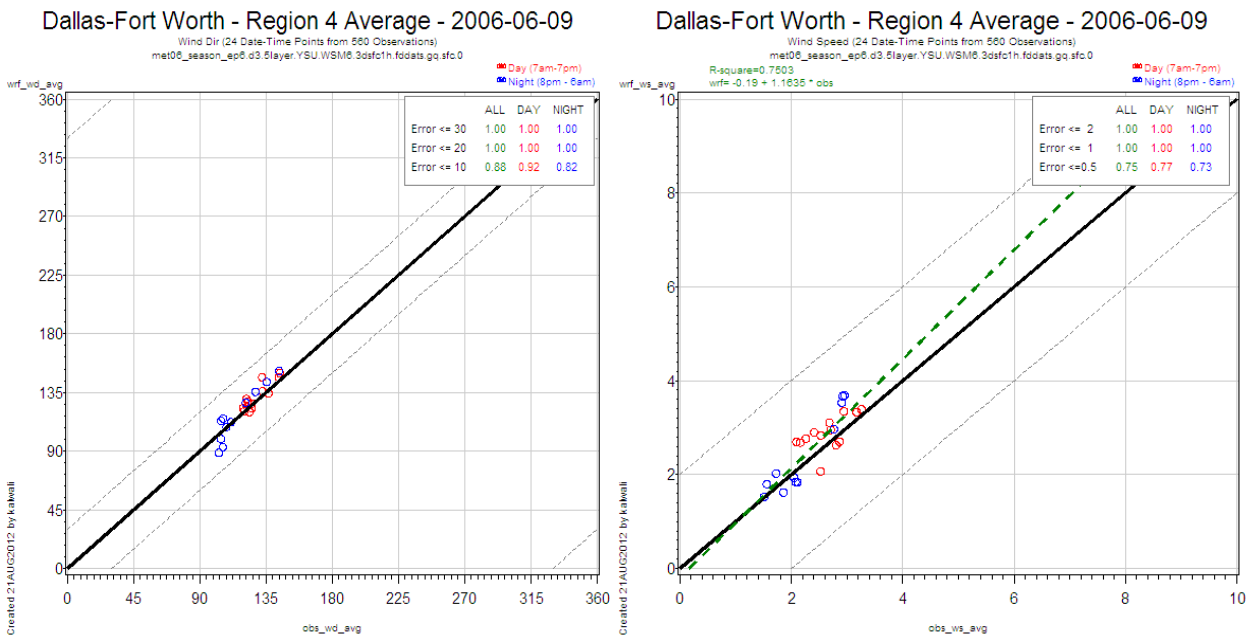

Figure 4-6: June 9, 2006 Wind Direction and Speed Scatter Plots

A comparison of cloud optical depth calculated by the WRF to CAMx converter (WRFCAMx) and GOES cloud fraction on this day Figure 4-7: June 9, 2006 WRFCAMx Cloud Optical Depth and GOES Cloud Fraction shows good agreement between model and observed data. In addition to generally light winds, the lightly scattered clouds were conducive to ozone formation.

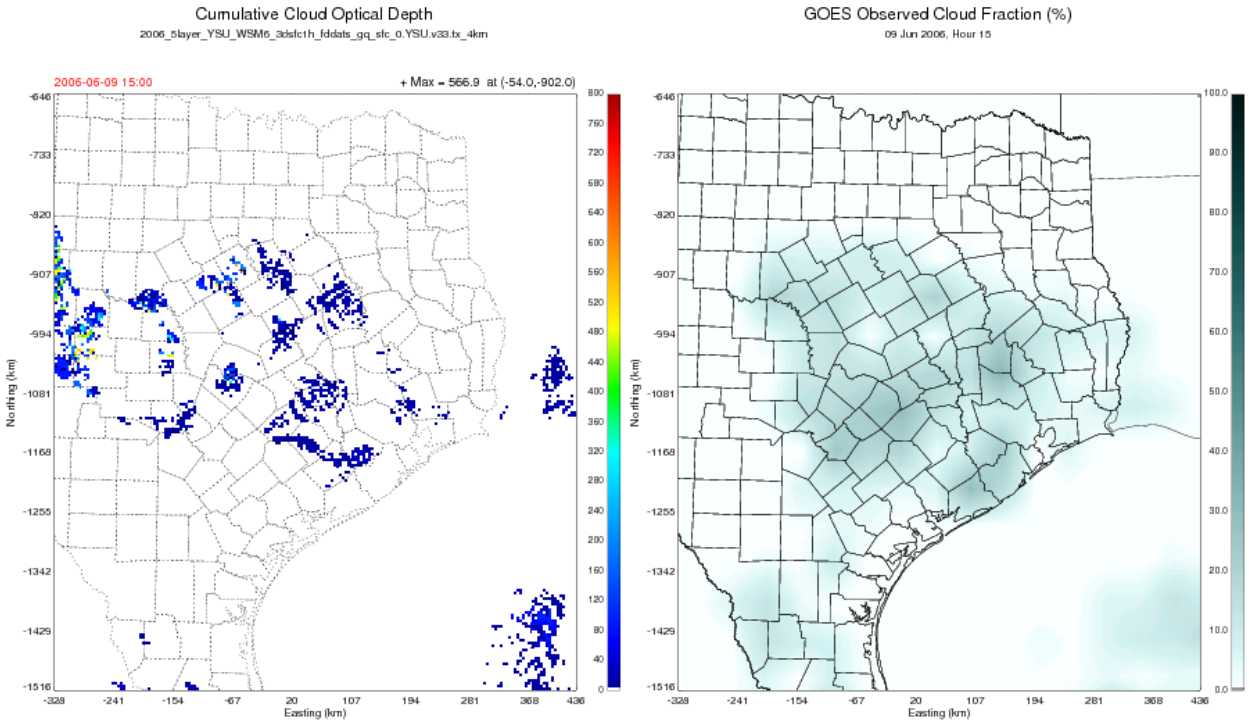

Figure 4-7: June 9, 2006 WRFCAMx Cloud Optical Depth and GOES Cloud Fraction

Aloft, WRF resolved much of the flow and PBL structure at the Cleburne profiler Figure 4-8: Time-height plot for the Cleburne Profiler on June 9, 2006 shows winds were generally from the southeast and 10 m/s or less above the surface. WRF captures these winds well. The model does not capture the morning jump in the PBL at 9 CST but matches the mid-day peak very well.

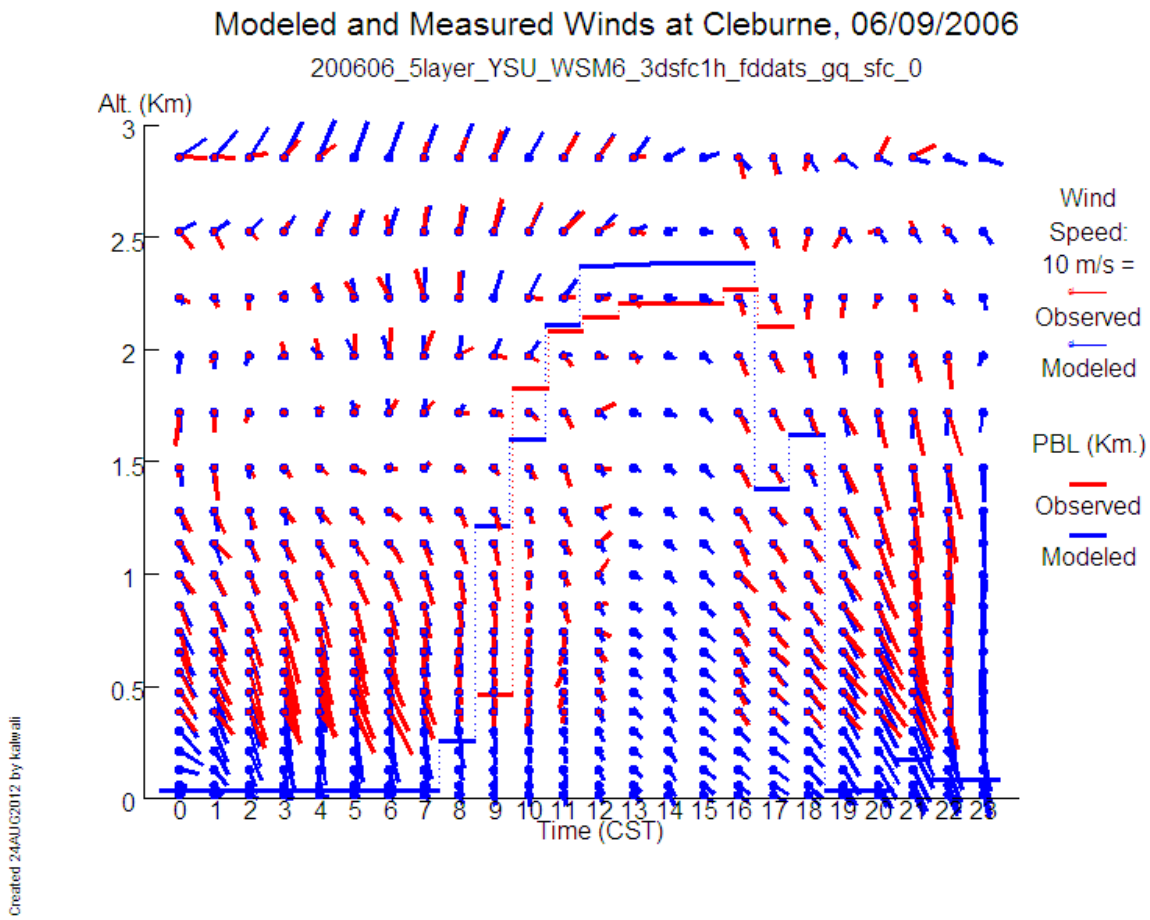

Figure 4-8: Time-height plot for the Cleburne Profiler on June 9, 2006

4.3 June 13, 2006 Performance Evaluation

Seven monitors recorded exceedances of the 1997 eight-hour ozone NAAQS on June 13, 2006. The peak eight-hour ozone, 98 ppb, was measured at the Cleburne and Midlothian Tower monitors on the southern side of the DFW. The major weather pattern along the Gulf of Mexico was Tropical Storm Alberto, which made landfall in northwest Florida on this day. The main flow on the northwest side of this low pressure system brought north to northeast winds towards Texas. A weak cold front had also passed through DFW, bringing northeast winds on the back side. The skies were generally clear with temperatures in the upper 80s.

WRF did a good job replicating the wind and temperature observations on this day as the percent of hours within the error benchmarks was very high on average and at most monitors Table 4-3: June 13, 2006 Meteorological Modeling Percent Accuracy. The wind direction and speed scatter plots, Figure 4-9: June 13, 2006 Wind Direction and Speed Scatter Plots, shows winds only from the northeast (0 – 90 degrees) at speeds less than 5 m/s. The scatter is small and almost all points fall along the one-to-one line.

Table 4-3: June 13, 2006 Meteorological Modeling Percent Accuracy

DFW Area	Wind Direction (°) Error ≤ 30 / 20 / 10	Wind Speed (m/s) Error ≤ 2 / 1 / 0.5	Temperature (°C) Error ≤ 2 / 1 / 0.5
Area Average	100 / 96 / 67	100 / 96 / 67	58 / 21 / 04

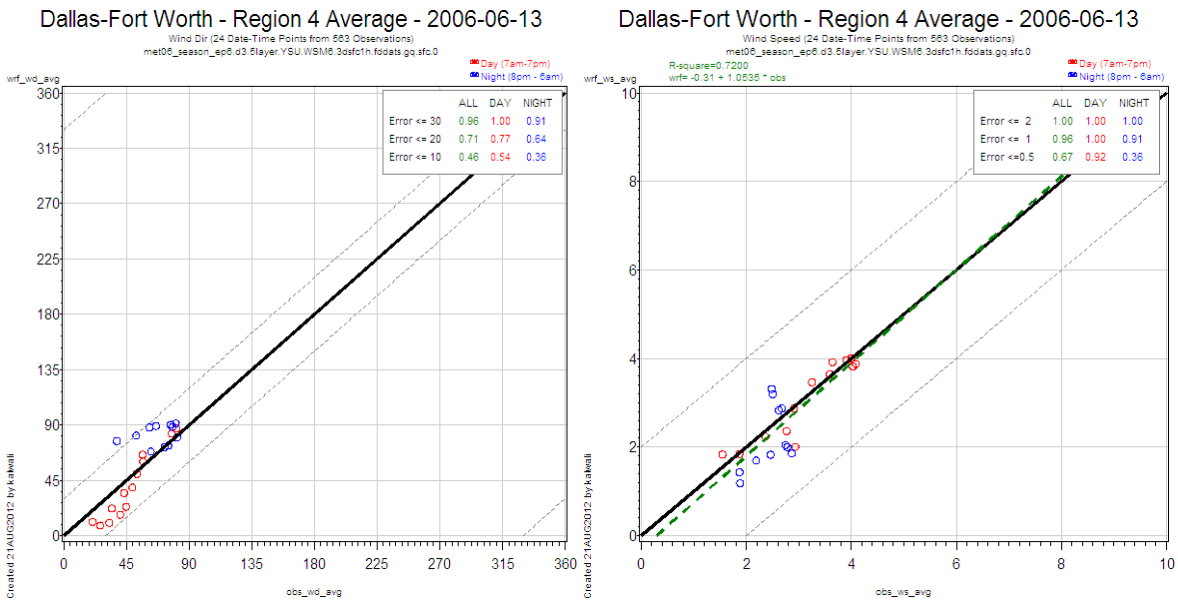

Figure 4-9: June 13, 2006 Wind Direction and Speed Scatter Plots

One possible impact of meteorological performance displayed in the scatter plots above Figure 4-9 is the domain-wide counterclockwise bias for night time hours. During the day, direction is biased slightly clockwise. This feature can be compared with the Cleburne profiler data below Figure 4-11: Time-height plot for the Cleburne Profiler on June 13, 2006. In general, though this day shows good domain-wide performance for these two metrics.

As with the scatter plots, cloud optical depth displays good model performance Figure 4-10: June 13, 2006 WRFCAMx Cloud Optical Depth and GOES Cloud Fraction with only light clouds southeast of DFW and along the Gulf coast.

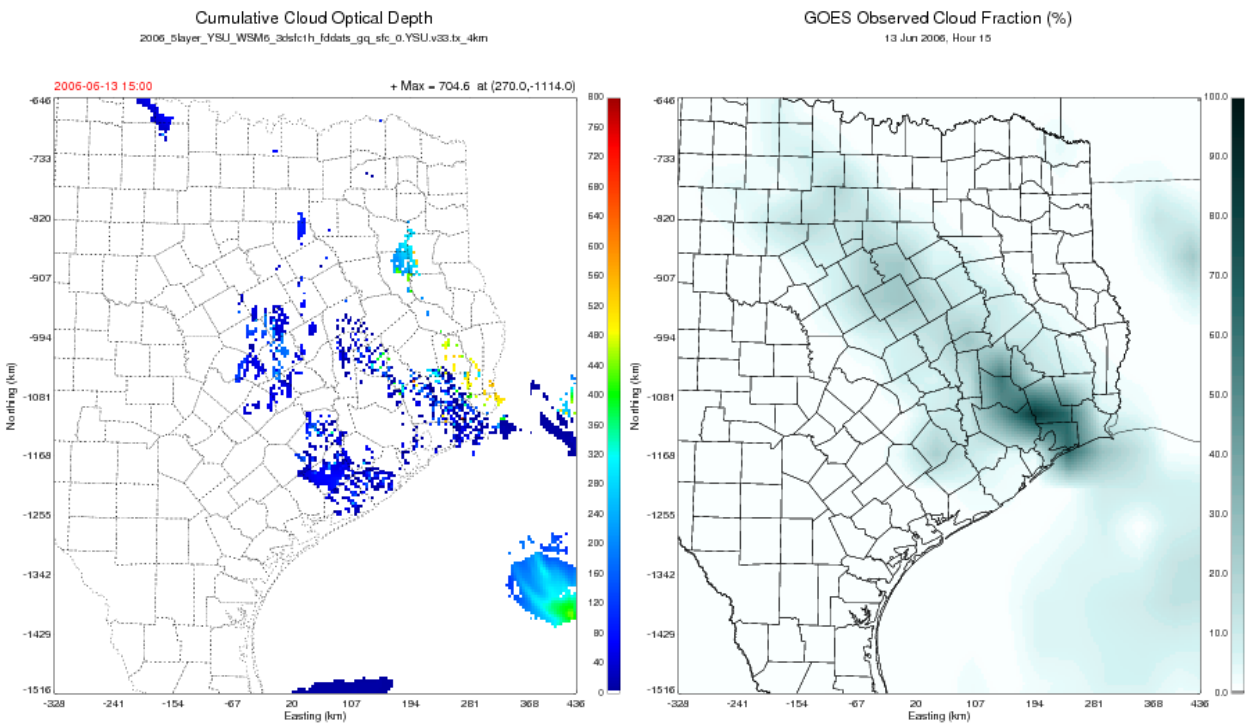

Figure 4-10: June 13, 2006 WRFCAMx Cloud Optical Depth and GOES Cloud Fraction

At the Cleburne profiler, the model simulates the wind speed and direction throughout the 3 km depth of the observations very well as shown below in Figure 4-11. As the day progresses, the wind shifts aloft from the east in the morning to the northeast in the afternoon. The model captures this shift well. The peak mixing is well approximated by the profiler data.

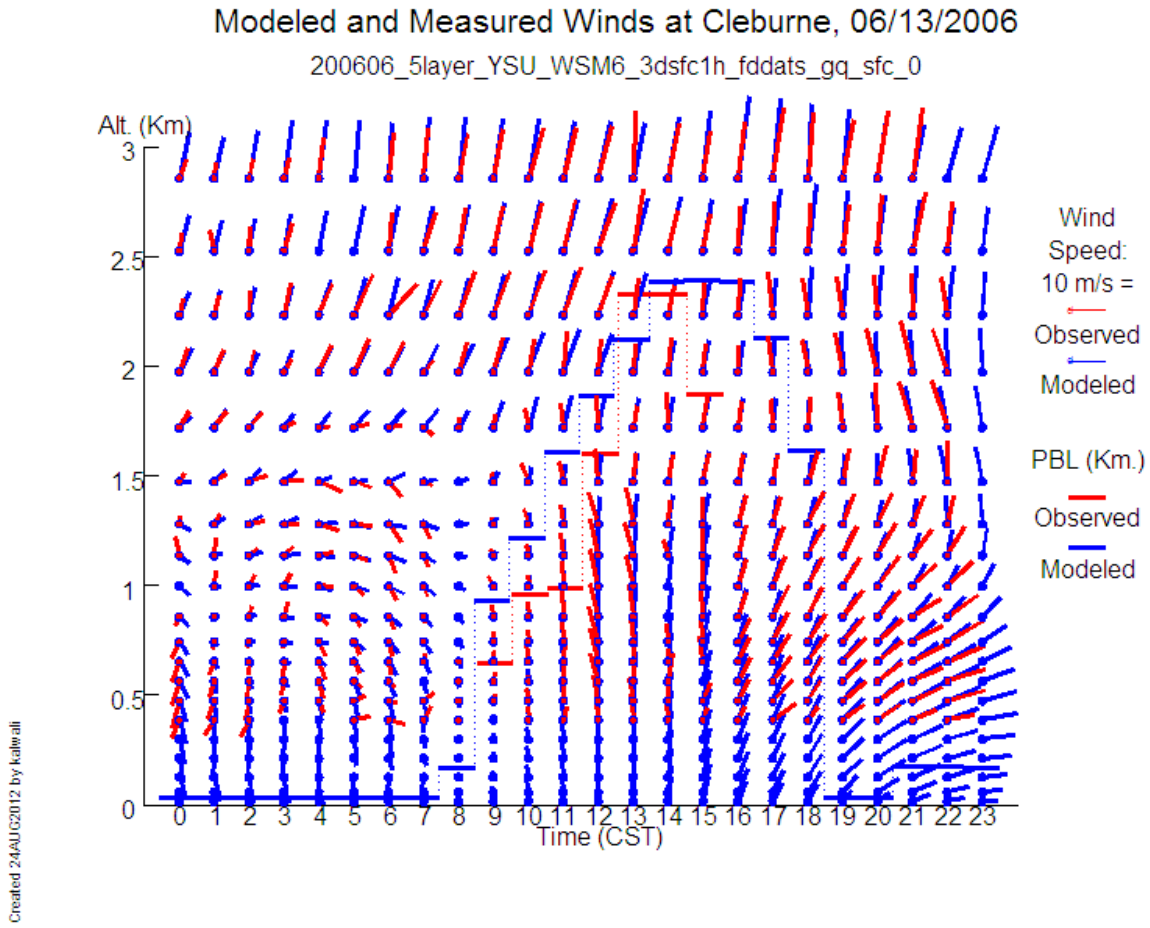

Figure 4-11: Time-height plot for the Cleburne Profiler on June 13, 2006

4.4 June 14, 2006 Performance Evaluation

The post-frontal regime continued on June 14, 2006 with east to southeast winds flowing for most of the day. Long range 48-hour backward trajectories (not shown) exhibit flow from the direction of the Ohio Valley. Those types of conditions can bring elevated background ozone concentrations, along with the observed clear skies and temperatures in the low 90s. Six monitors on the west side of DFW exceeded 84 ppb on this day, with a peak of 107 ppb at Eagle Mountain Lake. Wind and temperature performance on this day according to the error benchmarks were excellent Table 4-4: June 14, 2006 Meteorological Modeling Percent Accuracy. The scatter plots also show the model replicated the observed wind direction and speed very well in Figure 4-12: June 14, 2006 Wind Direction and Speed Scatter Plots.

Table 4-4: June 14, 2006 Meteorological Modeling Percent Accuracy

DFW Area	Wind Direction (°) Error ≤ 30 / 20 / 10	Wind Speed (m/s) Error ≤ 2 / 1 / 0.5	Temperature (°C) Error ≤ 2 / 1 / 0.5

DFW Area	Wind Direction (°) Error ≤ 30 / 20 / 10	Wind Speed (m/s) Error ≤ 2 / 1 / 0.5	Temperature (°C) Error ≤ 2 / 1 / 0.5
Area Average	100 / 100 / 88	100 / 100 / 83	96 / 25 / 08

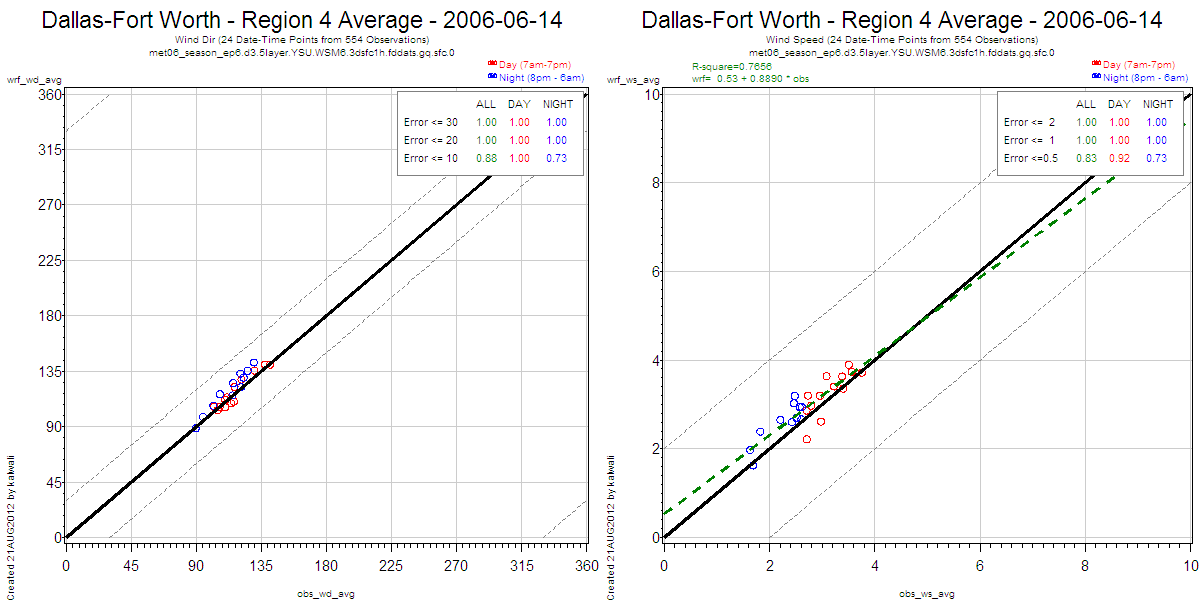

Figure 4-12: June 14, 2006 Wind Direction and Speed Scatter Plots

This episode day only had light clouds along the Texas coast, and WRF modeling replicated the clear skies the predominated over north central Texas.Figure 4-13: June 14, 2006 WRFCAMx Cloud Optical Depth and GOES Cloud Fraction.

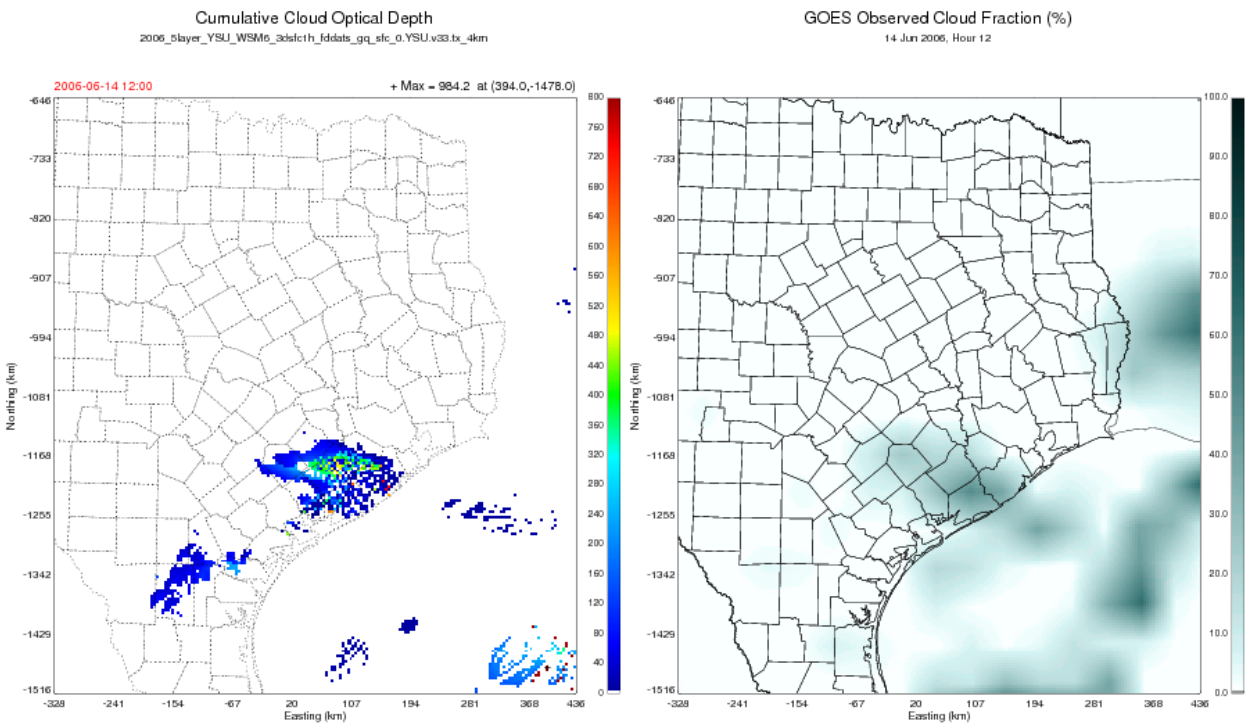

Figure 4-13: June 14, 2006 WRFCAMx Cloud Optical Depth and GOES Cloud Fraction

As on June 13, 2006, WRF replicates the upper air winds very well in comparison to the Cleburne profiler data Figure 4-14: Time-height plot for the Cleburne Profiler on June 14, 2006. Although the model displayed some clockwise bias in wind direction during the morning hours aloft, daytime wind speed and direction within the modeled boundary layer were very well captured. Observations of the PBL were not available on this day.

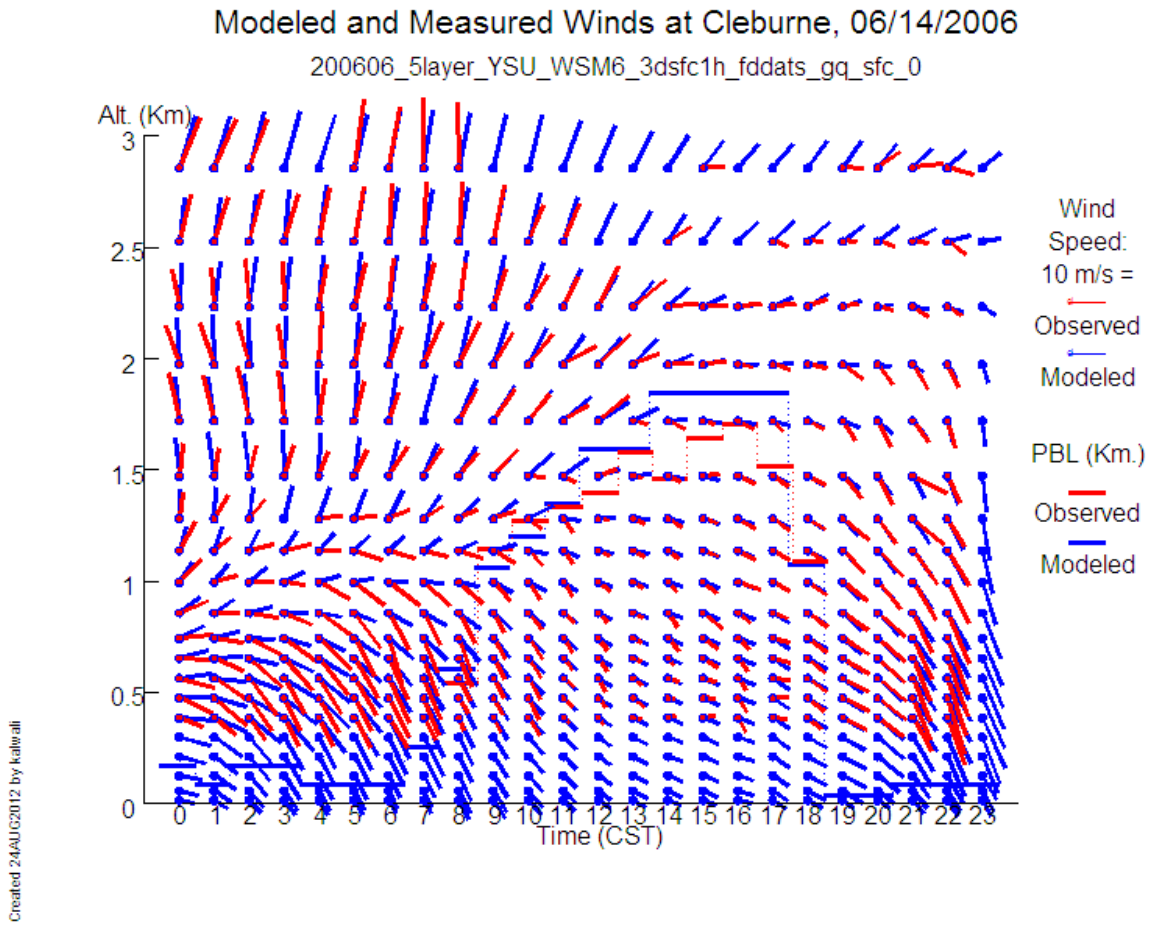

Figure 4-14: Time-height plot for the Cleburne Profiler on June 14, 2006

4.5 June 18, 2006 Performance Evaluation

June 18, 2006 was a difficult day for the model to replicate. The previous day had strong southerly flow with significant cloud cover. A low pressure system came through the area that brought brief northwest winds that stalled and then slowly reversed to come from the south. In the late afternoon weak southeast winds returned. Eight monitors exceeded the 84 ppb standard with the peak of 97 ppb at Denton Airport South.

As Table 4-5: June 18, 2006 Meteorological Modeling Percent Accuracy shows, the model had difficulty in simulating the wind directions. The wind speeds were very slow on this day (and well replicated), which should make the wind direction less important for ozone and ozone precursor transport. During some hours though, WRF wind direction was off by more than 100 degrees as shown in Figure 4-15: June 18, 2006 Wind Direction and Speed Scatter Plots.

Table 4-5: June 18, 2006 Meteorological Modeling Percent Accuracy

DFW Area	Wind Direction (°) Error ≤ 30 / 20 / 10	Wind Speed (m/s) Error ≤ 2 / 1 / 0.5	Temperature (°C) Error ≤ 2 / 1 / 0.5
Area Average	58 / 46 / 29	100 / 100 / 71	100 / 58 / 13

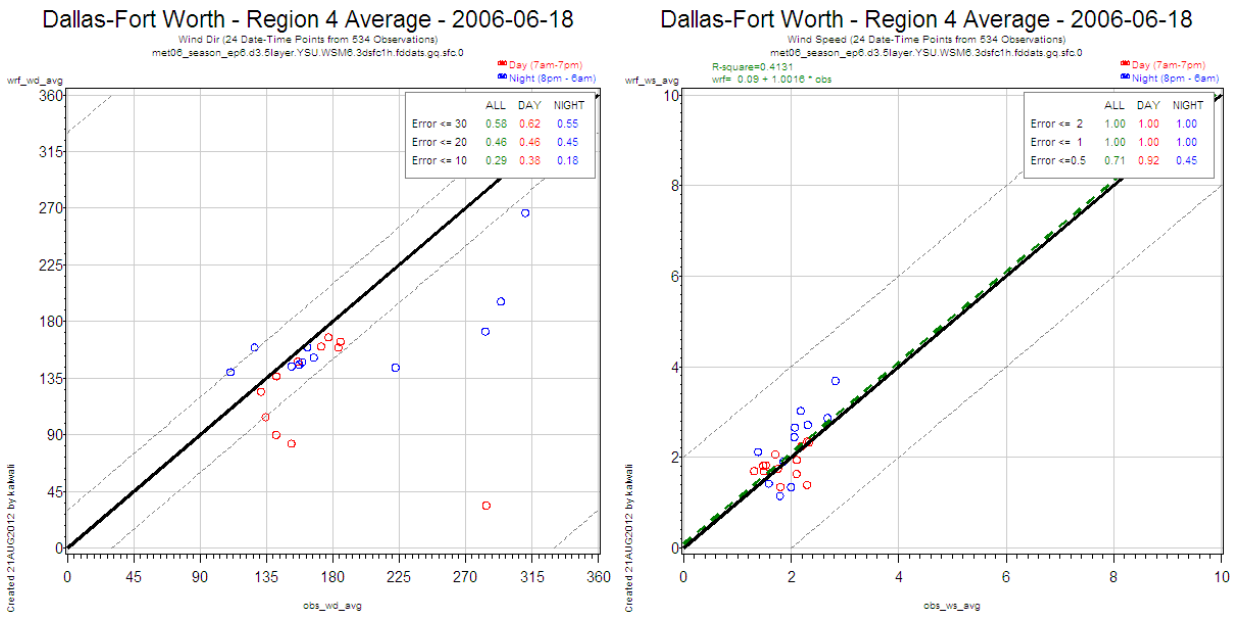

Figure 4-15: June 18, 2006 Wind Direction and Speed Scatter Plots

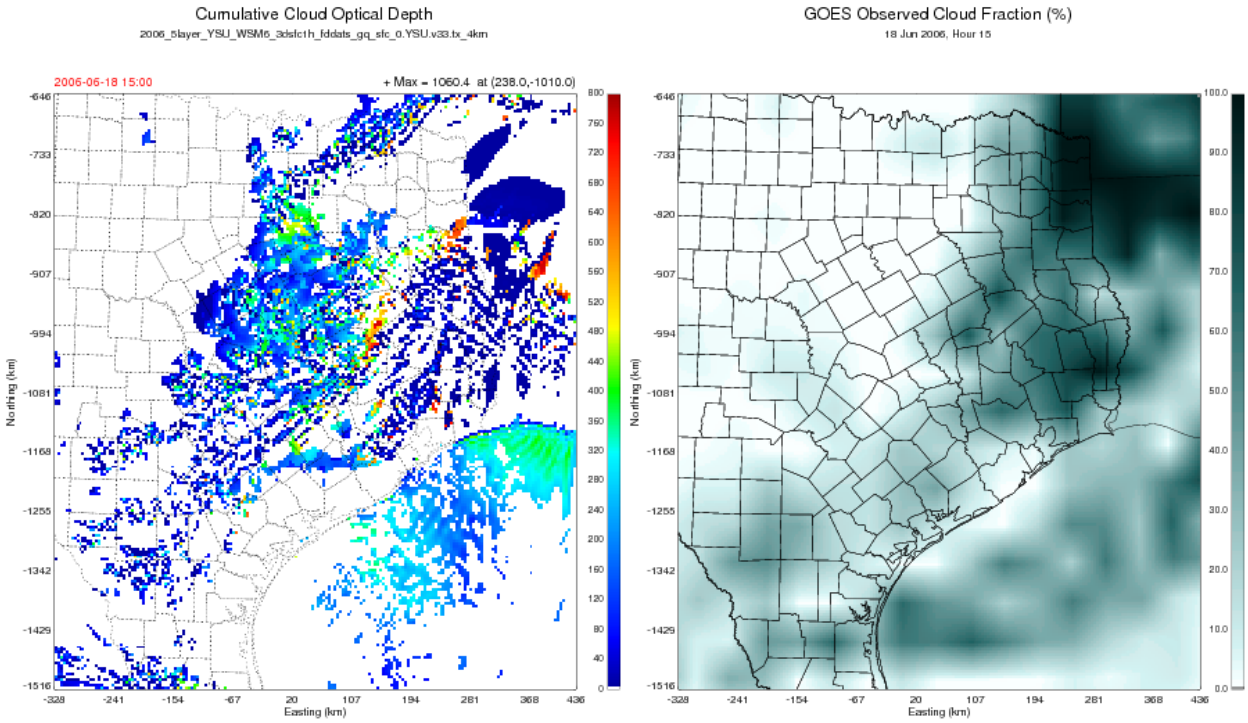

Figure 4-16: June 18, 2006 WRFCAMx Cloud Optical Depth and GOES Cloud Fraction

Figure 4-16 indicates the importance of WRF modeling clouds properly, even though the WRFCAMx cloud optical depth roughly matches the GOES cloud fraction. The cloudy skies over

DFW were considered cloudy in the model and the boundary between cloudy and clear skies would have been further to the east.

WRF does a respectable job of replicating the upper air winds at the Cleburne profiler, especially in the afternoon. Figure 4-17Figure 4-17: Time-height plot for the Cleburne Profiler on June 18, 2006. The morning winds are not as well represented during the northeasterly flow. The model captures the growth, peak, and collapse of the PBL.

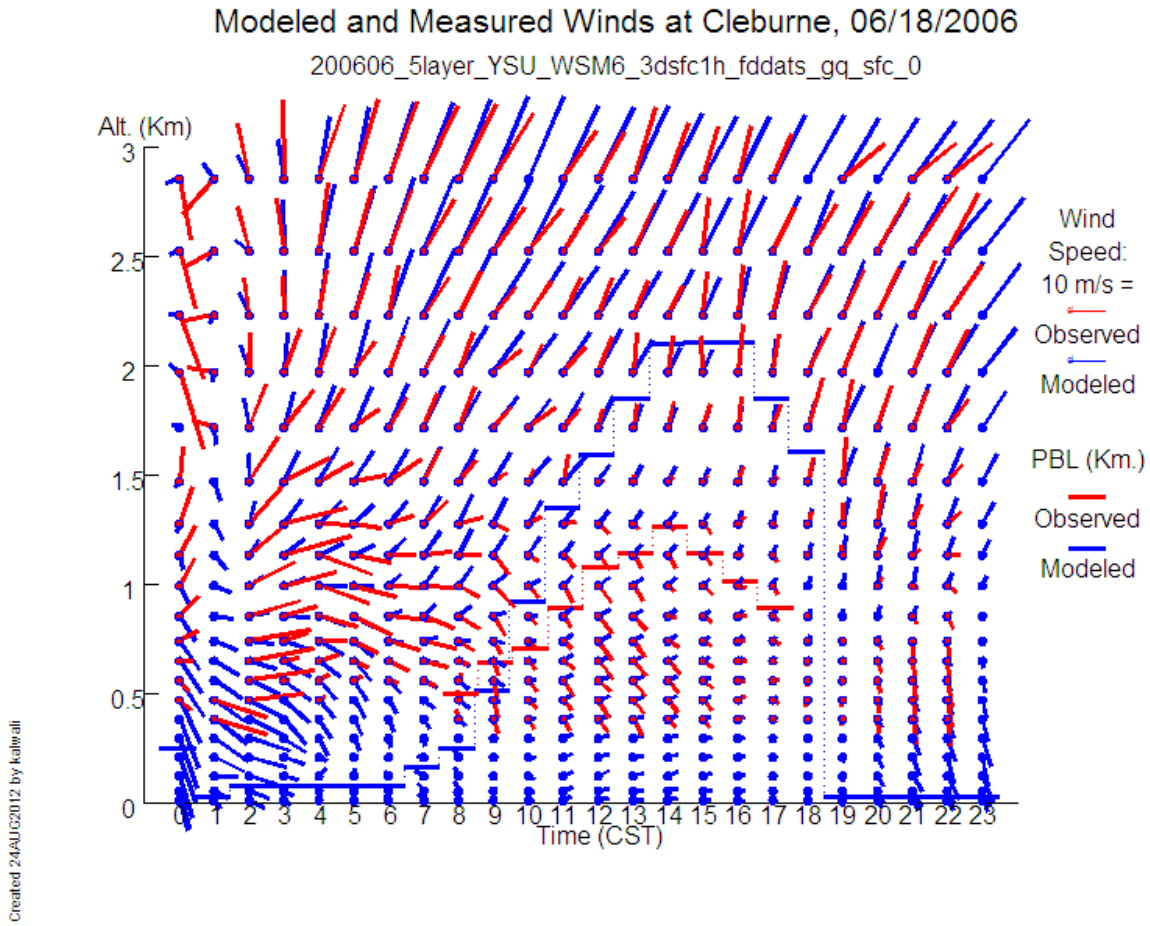

Figure 4-17: Time-height plot for the Cleburne Profiler on June 18, 2006

4.6 June 28, 2006 Performance Evaluation

High pressure was centered to the east of Texas on June 28, 2006, which brought light southerly winds. Skies were generally clear with temperatures in the low 90s. Six sites on the northwest and north side of DFW measured eight-hour ozone exceedances, with the peak of 98 ppb at Eagle Mountain Lake. Elevated background ozone may have contributed to the exceedances as upwind sites such as Kaufman measured 70 – 75 ppb.

WRF replicated the overall pattern of winds on this day, though the wind direction statistics suffered somewhat due to the meandering southerly winds over the course of the day Table 4-6: June 28, 2006 Meteorological Modeling Percent Accuracy; Figure 4-18: June 28, 2006 Wind Direction and Speed Scatter Plots. Wind speed accuracy though was very good.

Table 4-6: June 28, 2006 Meteorological Modeling Percent Accuracy

DFW Area	Wind Direction (°) Error ≤ 30 / 20 / 10	Wind Speed (m/s) Error ≤ 2 / 1 / 0.5	Temperature (°C) Error ≤ 2 / 1 / 0.5
Area Average	83 / 67 /58	100 / 100 / 67	58 / 25 / 08

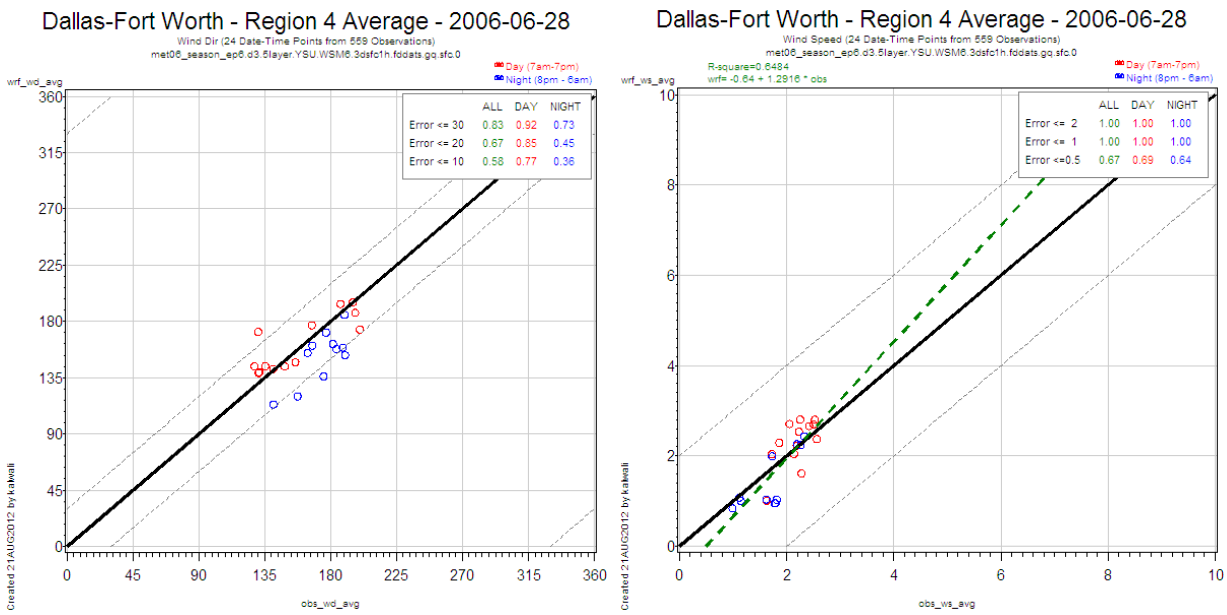

Figure 4-18: June 28, 2006 Wind Direction and Speed Scatter Plots

In Figure 4-19: June 28, 2006 WRFCAMx Cloud Optical Depth and GOES Cloud Fraction clouds were scattered and largely confined to the central part of the state. Generally light cloud cover over north central Texas was reasonably well captured

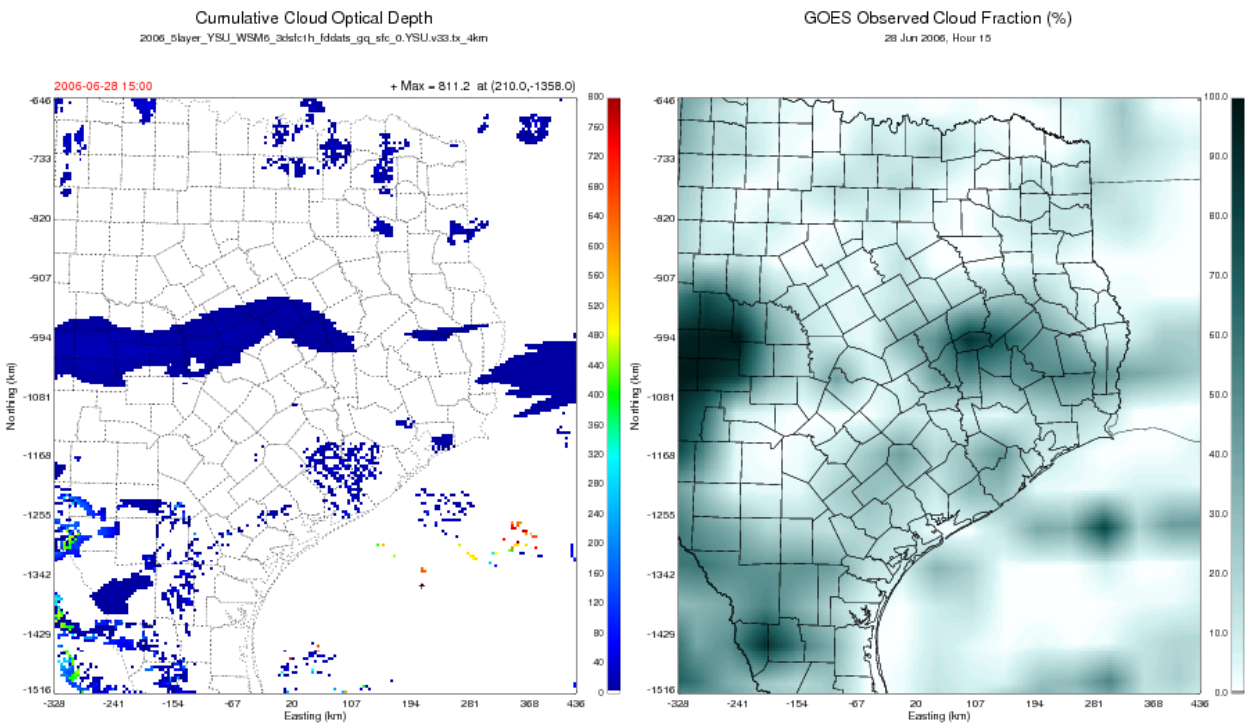

Figure 4-19: June 28, 2006 WRFCAMx Cloud Optical Depth and GOES Cloud Fraction

At the Cleburne profiler, WRF replicates the aloft winds well Figure 4-20: Time-height plot for the Cleburne Profiler on June 28, 2006. The reduction in wind speeds from late morning to mid-afternoon was captured appropriately. Wind speeds at all levels largely matched profiler data.

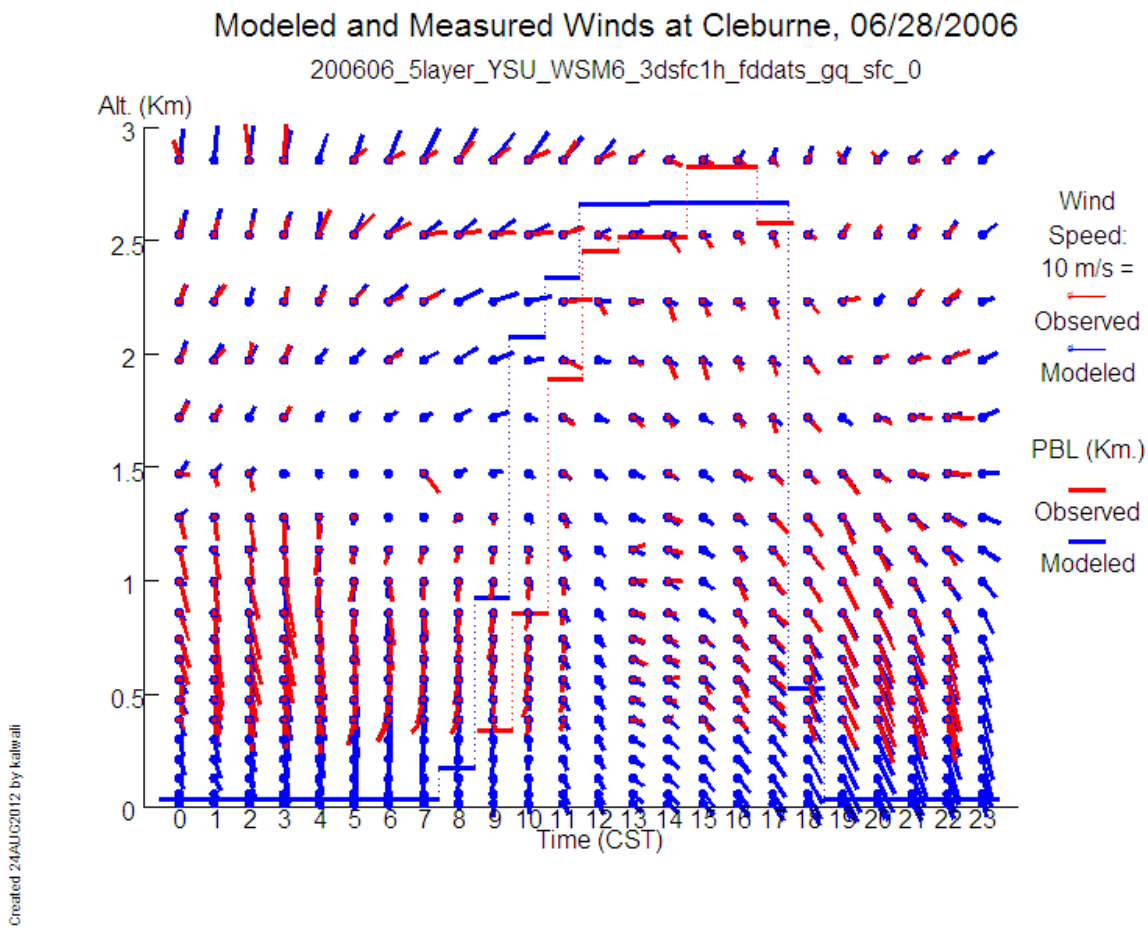

Figure 4-20: Time-height plot for the Cleburne Profiler on June 28, 2006

4.7 August 15-September 15, 2006 Episode Performance Evaluation

The August 15-September 15 2006 episode had twelve days (out of 31) with an observed eight-hour ozone exceedance. Eight of those days had more than five DFW monitors exceeding 75 ppb. On the days of August 31st and September 1st, fourteen monitors and seventeen monitors (out of twenty) respectively, had exceedances.

In contrast to the June 2006 episode, several weak surface fronts were associated with high pressure aloft during August high episode days. This broad feature generated many cloudy days, especially along the Texas coast and west Texas, but north central Texas clouds were sparse enough with light winds to produce ozone. However, even with generally good predicted cloud coverage on August 22nd and 23rd ozone values were over predicted. September had more pronounced northerly flow and greater cloud coverage, but September 1st proved to have the highest eight hour ozone during this episode.

The WRF modeling was evaluated by comparing the hourly modeled and measured wind speed, wind direction, and temperature for all monitors in the DFW area Figure 4-21: August 2006 Meteorological Modeling Performance exhibits the percent of hours for which the average absolute difference between the modeled and measured wind speed and direction, for specific monitors and a DFW area average, was within the specified accuracy benchmarks (e.g., wind speed difference less than or equal to two meters per second: WSPD ≤ 2 m/s).

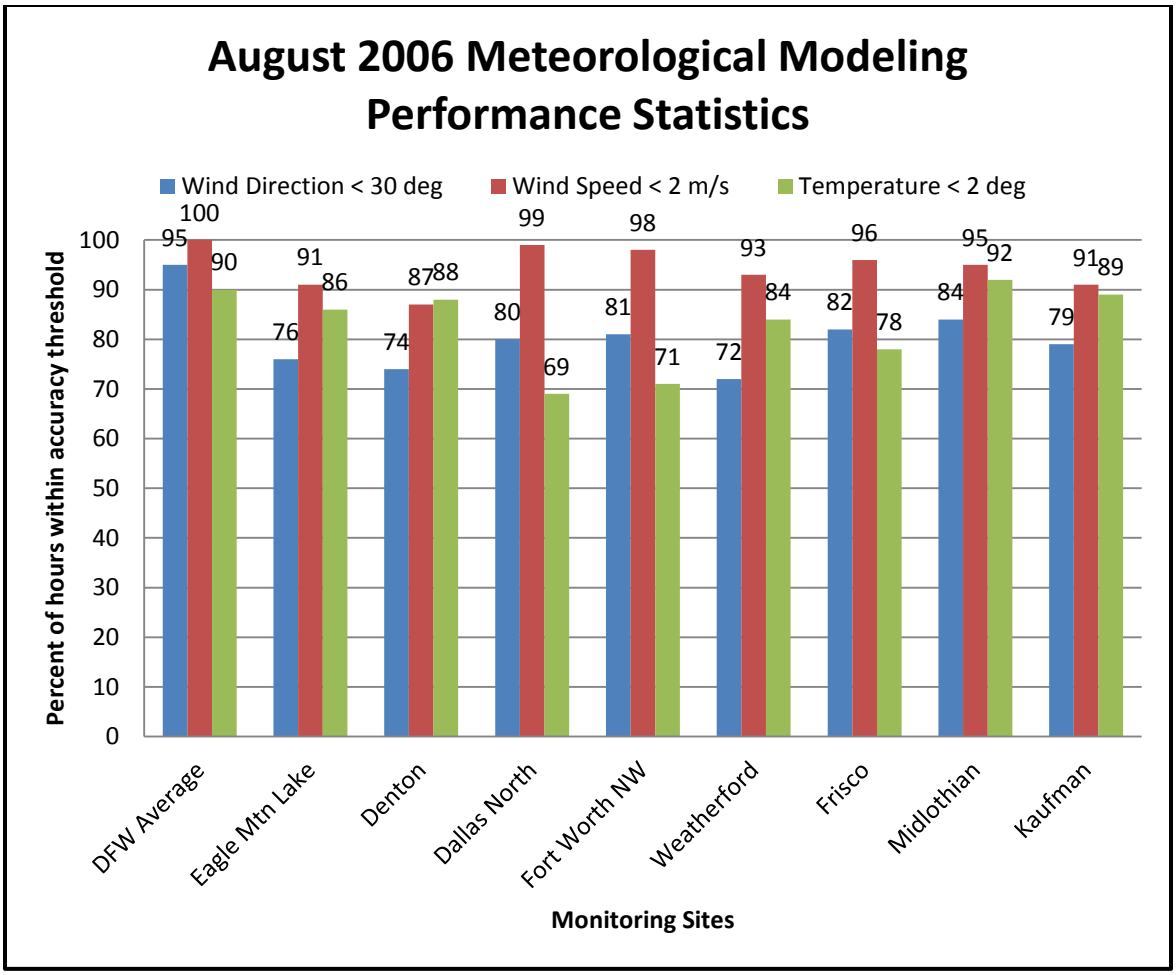

Figure 4-21: August 2006 Meteorological Modeling Performance

Table 4-7: August 2006 DFW Meteorological Modeling Percent Accuracy indicates that across all monitors in the DFW are there was similar performance across all thresholds of accuracy. Although wind speed accuracy may not have matched the June 2006 episode, there was perhaps a larger degree of consistency

Table 4-7: August 2006 DFW Meteorological Modeling Percent Accuracy

DFW Area	Wind Direction (°) Error ≤ 30 / 20 / 10	Wind Speed (m/s) Error ≤ 2 / 1 / 0.5	Temperature (°C) Error ≤ 2 / 1 / 0.5
Area Average	95 / 85 / 62	100 / 97 / 73	90 / 54 / 24
Eagle Mountain Lake	76 / 64 / 39	91 / 65 / 38	86 /48 / 27
Denton	74 / 63 /37	87 / 59 / 33	88 / 54/ 26
Dallas North	80 / 61 / 35	99 / 87 / 55	69 / 28 / 13
Fort Worth NW	81 / 69 / 43	98 / 77 /45	71 / 30 / 13
Weatherford	72 / 59 / 38	93 / 68 / 38	84 / 48 / 23
Frisco	82 / 69 / 48	96 / 69 / 40	78 / 45 / 21
Midlothian Tower	84 / 70 / 32	95 / 72 / 40	92 / 60 / 30
Kaufman	79 / 66 / 36	91 / 60 / 33	89 / 58 / 26

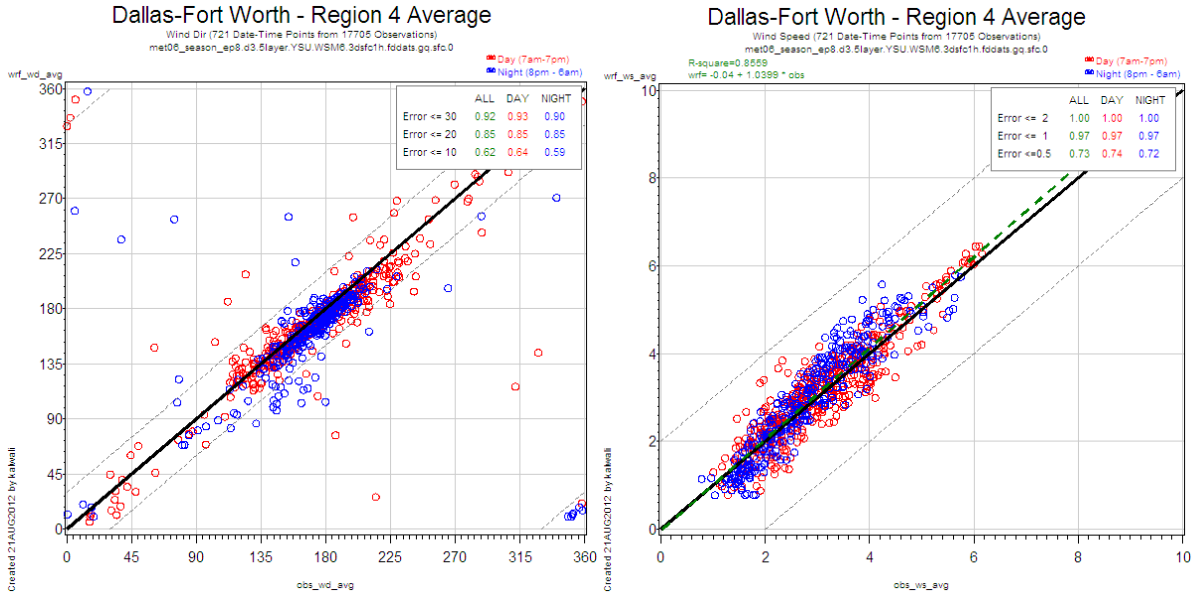

Figure 4-22: DFW August Average Wind Direction and Speed Scatter Plots

The WRF scatter plots Figure 4-22: DFW August Average Wind Direction and Speed Scatter Plots shown in and Figure 4-23: DFW August Average Wind Direction Time Series and Figure 4-24: DFW August Average Wind Speed Time Series display negligible bias through the entire month. As noted previously, model configuration was selected to focus on these meteorological variables. Temperature statistics reflect the use to use archived soil moisture from WRF model initialization rather than a more complicated land surface model.

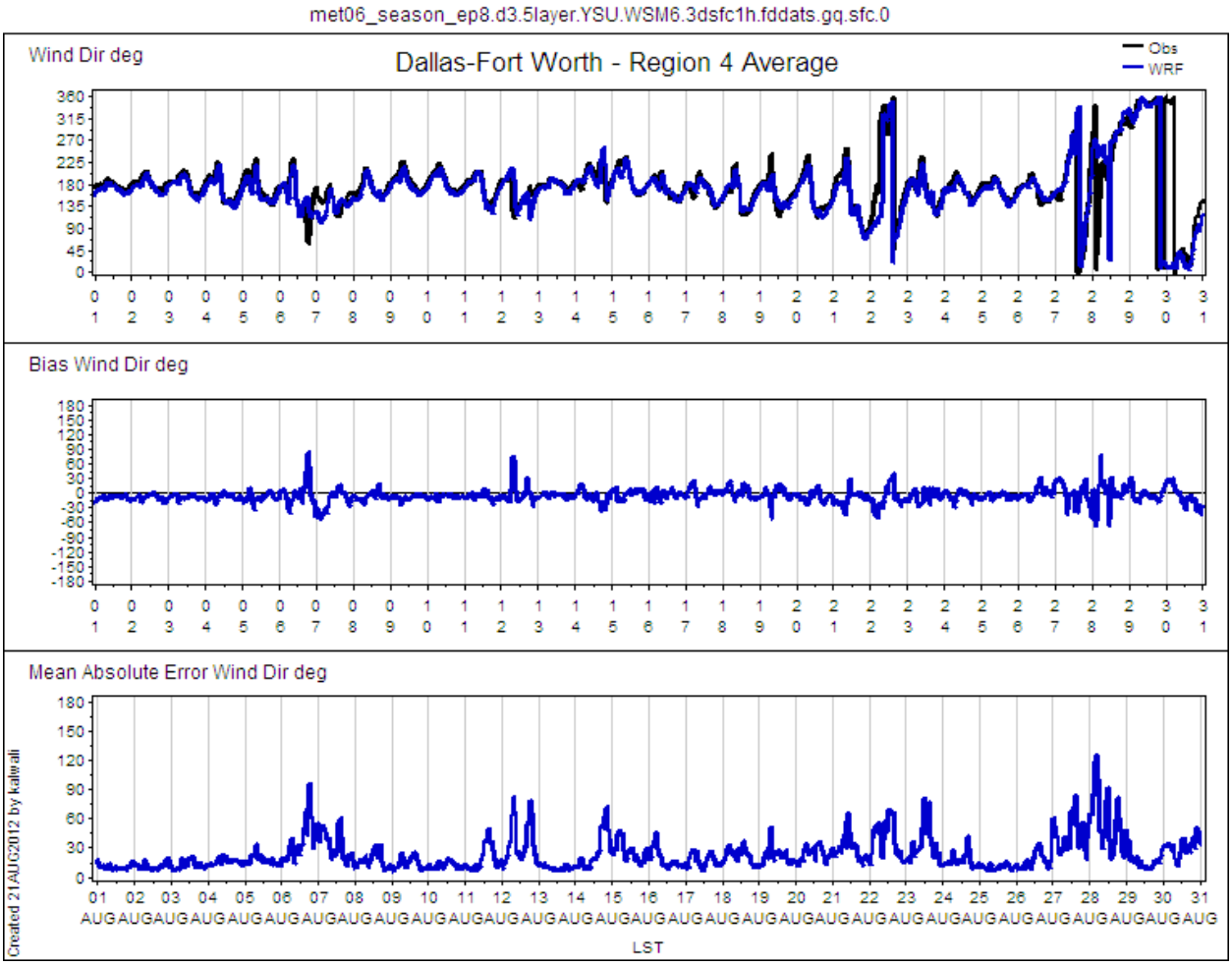

Figure 4-23: DFW August Average Wind Direction Time Series

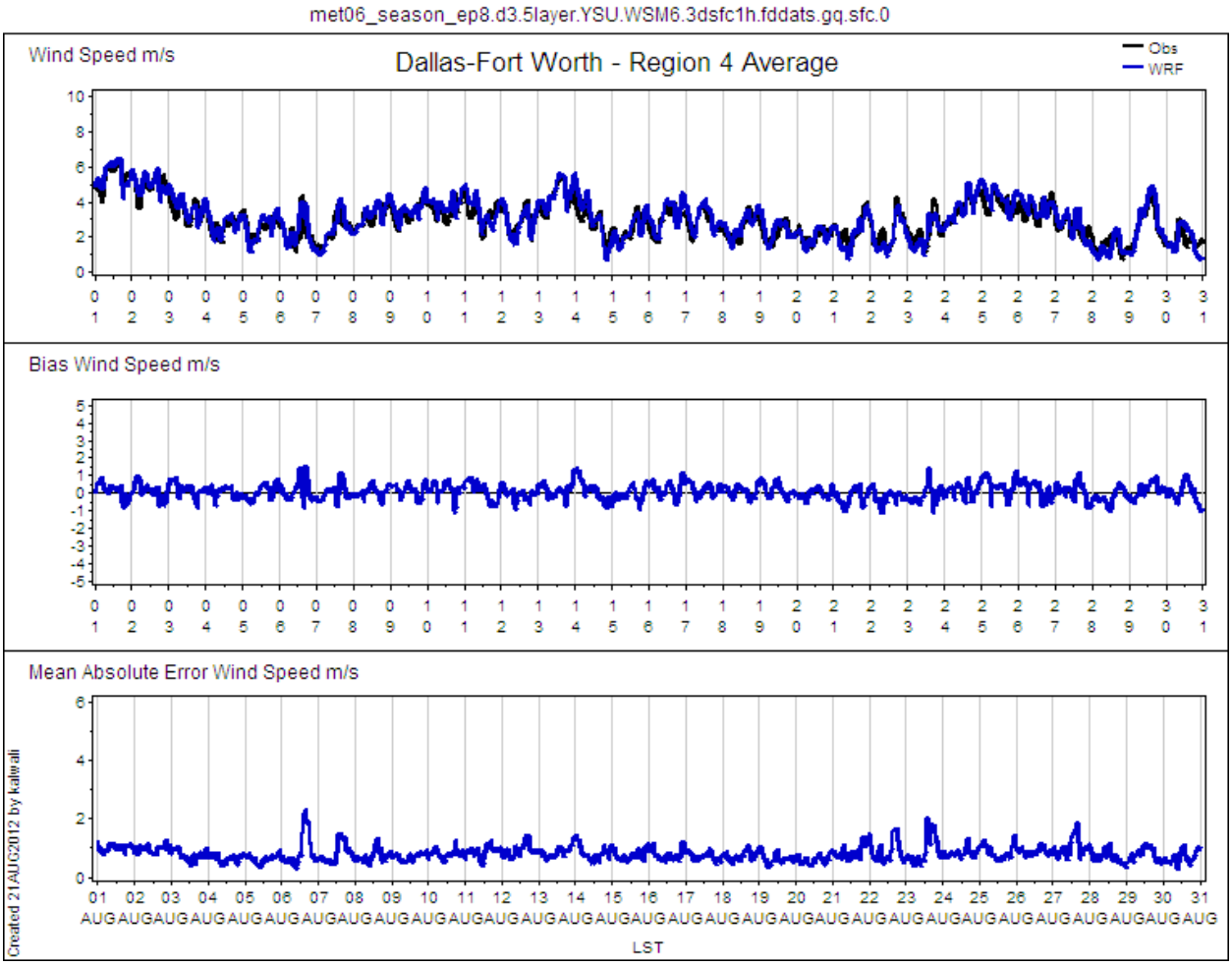

Figure 4-24: DFW August Average Wind Speed Time Series

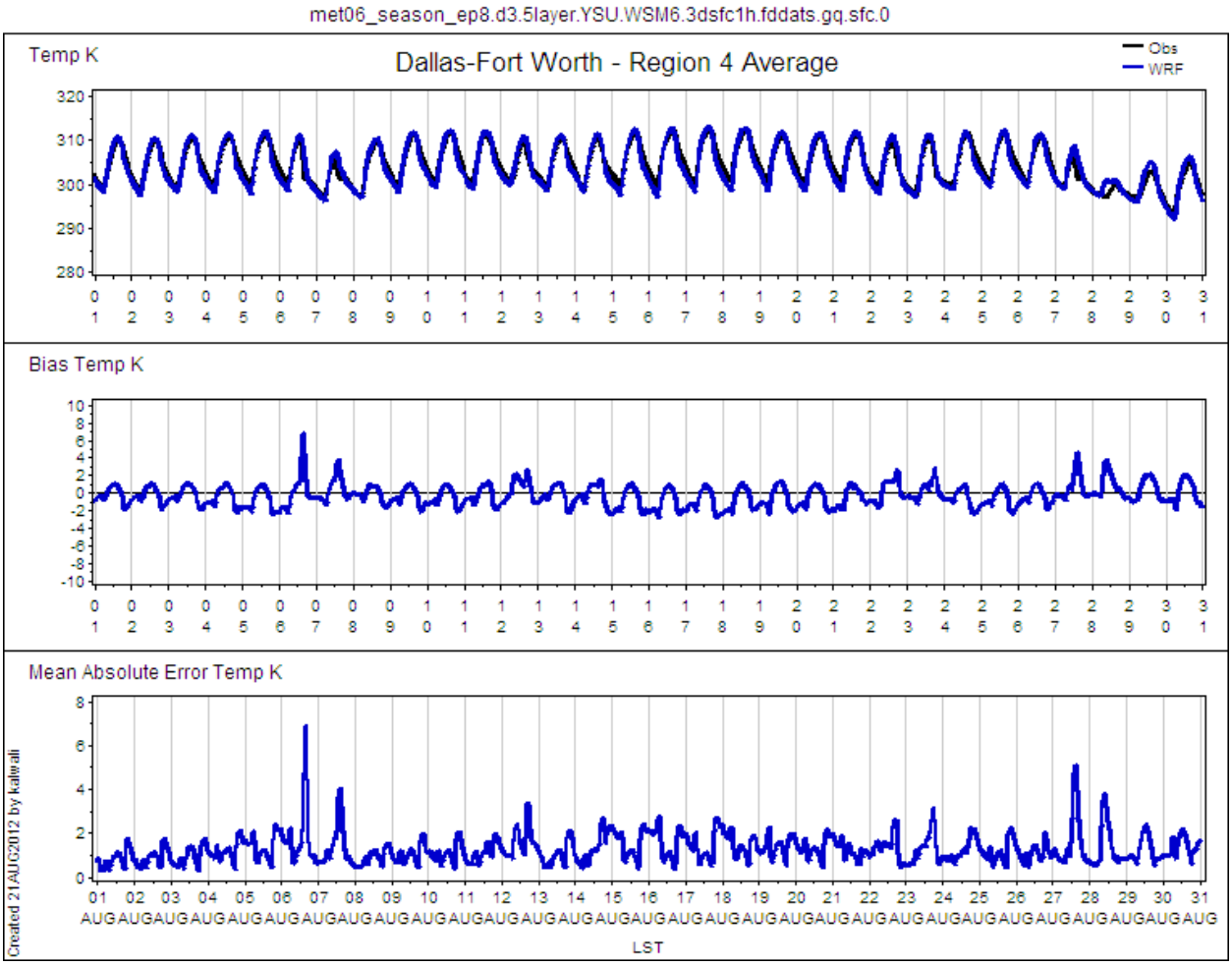

Figure 4-25: DFW August Average Temperature Time Series

The next series of figures and Table 4-8: September 2006 DFW Meteorological Modeling Percent Accuracy summarize WRF model performance during September 2006. Wind speeds were very well replicated. As shown in Figure 4-27: DFW September 2006 Average Wind Direction Time Series a series of frontal passages with pronounced northerly flow characterized much of this month. The post-frontal passage of August 30th was followed by high ozone on August 31st and September 1st. Other days with notable ozone – September, 7th and 8th as well as September 14th also followed this pattern. It is also important that these days also experienced relatively light wind speeds in contrast to other frontal system between September 22nd and 24th.

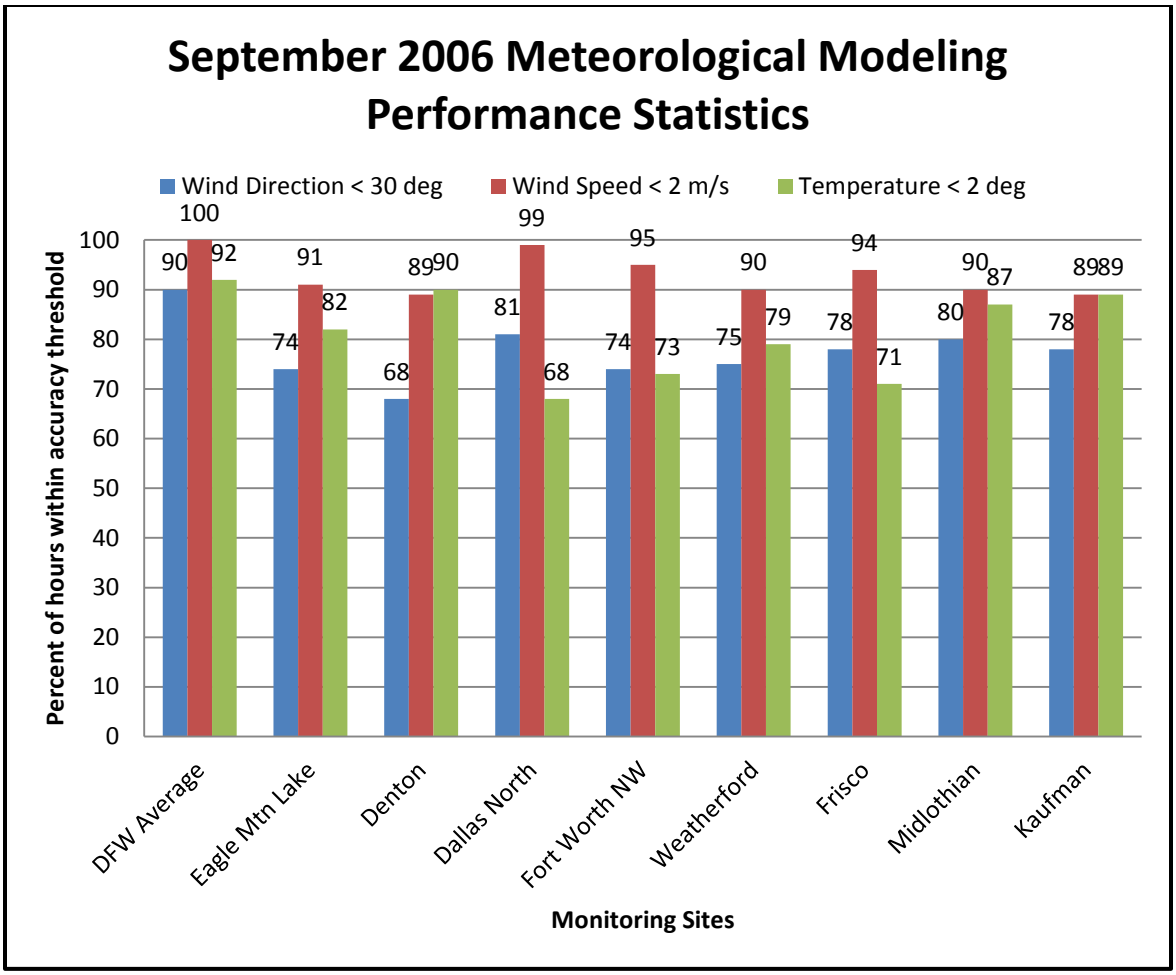

Figure 4-26: September 2006 Meteorological Modeling Performance

Table 4-8: September 2006 DFW Meteorological Modeling Percent Accuracy

DFW Area	Wind Direction (°) Error ≤ 30 / 20 / 10	Wind Speed (m/s) Error ≤ 2 / 1 / 0.5	Temperature (°C) Error ≤ 2 / 1 / 0.5
Area Average	90 / 80 / 63	100 / 91 / 65	92 / 50 / 22
Eagle Mountain Lake	74 / 64 / 40	91 / 64 / 31	82 /45 / 23
Denton	68 / 59 /41	89 / 62 / 36	90 / 57/ 30
Dallas North	81 / 70 / 43	99 / 86 / 55	68 / 30 / 13
Fort Worth NW	74 / 64 / 42	95 / 80 /49	73 / 35 / 16
Weatherford	75 / 64 / 40	90 / 61 / 34	79 / 47 / 24
Frisco	78 / 67 / 44	94 / 70 / 43	79 / 42 / 21
Midlothian Tower	80 / 70 / 44	90 / 64 / 36	71 / 41 / 23
Kaufman	78 / 64 / 38	89 / 64 / 39	87 / 51 / 29

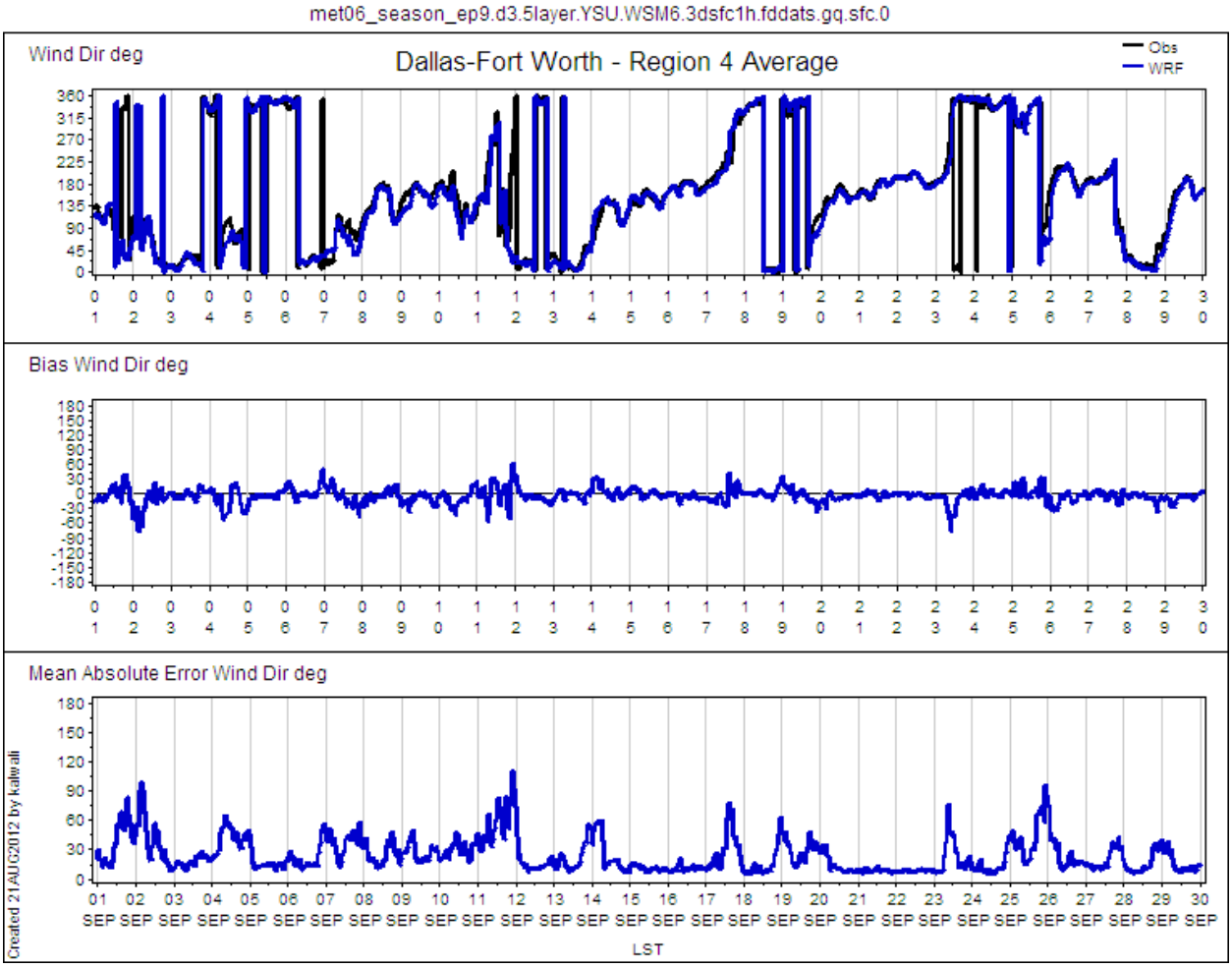

Figure 4-27: DFW September 2006 Average Wind Direction Time Series

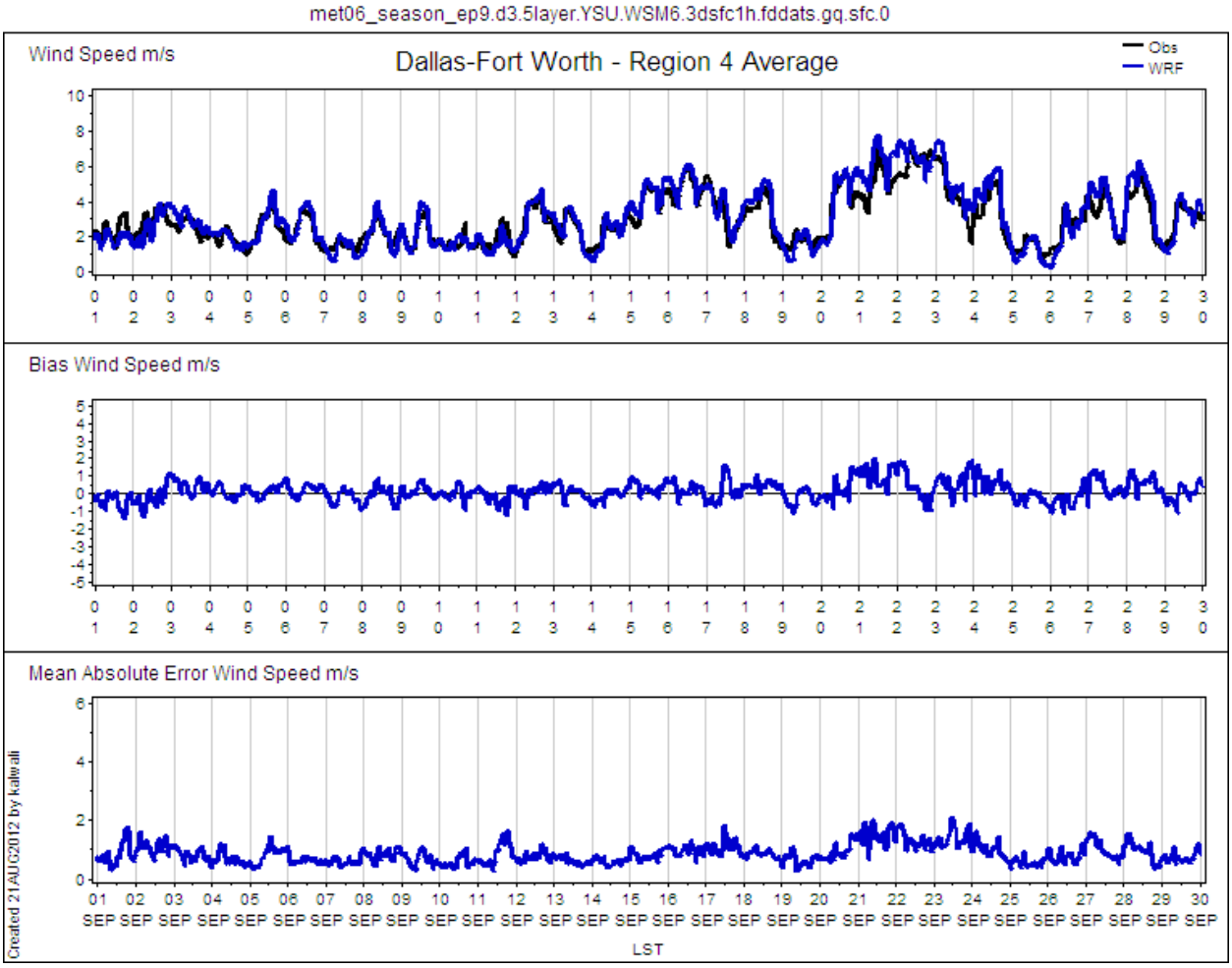

Figure 4-28: DFW September 2006 Average Wind Speed Time Series

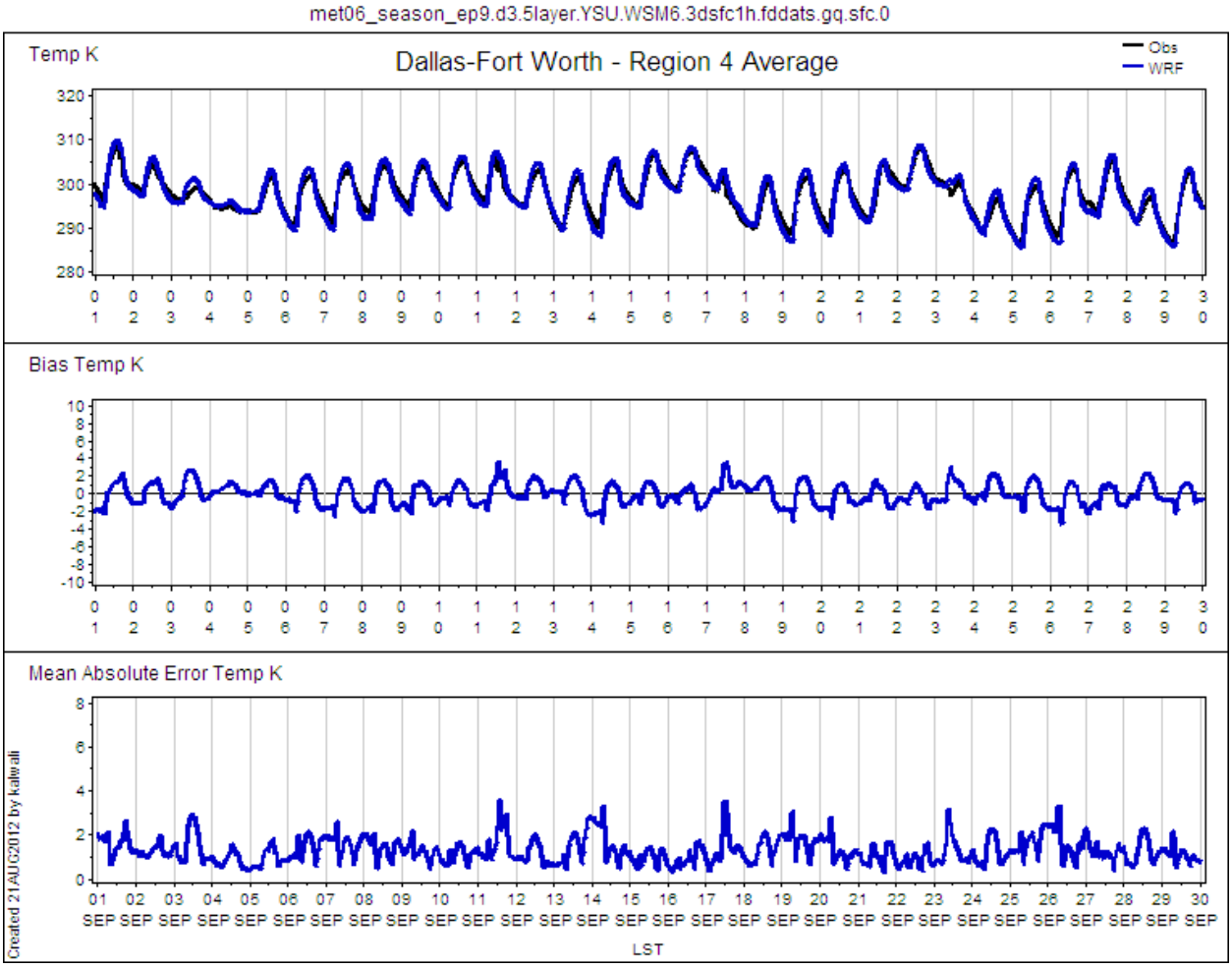

Figure 4-29: DFW September 2006 Average Temperature Time Series

4.8 August 21, 2006 Performance Evaluation

A weak cold front from the previous day became stationary on august 21, 2006, and although there were clouds to the east and north, the DFW area was largely cloud free. Generally, southerly flow veered from southwest to southeast during the daylight hours, before reversing again in the evening. Winds were very light through the day. Overall modeling accuracy was good as indicated in Table 4-9: August 21, 2006 Meteorological Modeling Percent Accuracy.

WRF wind direction as shown in Figure 4-30: August 21, 2006 Wind Direction and Speed Scatter Plots indicates a weak clockwise bias, but the wind speed exhibited almost no bias.

Table 4-9: August 21, 2006 Meteorological Modeling Percent Accuracy

DFW Area	Wind Direction (°) Error ≤ 30 / 20 / 10	Wind Speed (m/s) Error ≤ 2 / 1 / 0.5	Temperature (°C) Error ≤ 2 / 1 / 0.5
Area Average	96 / 88 / 33	100 / 100 / 71	100 / 50 / 17

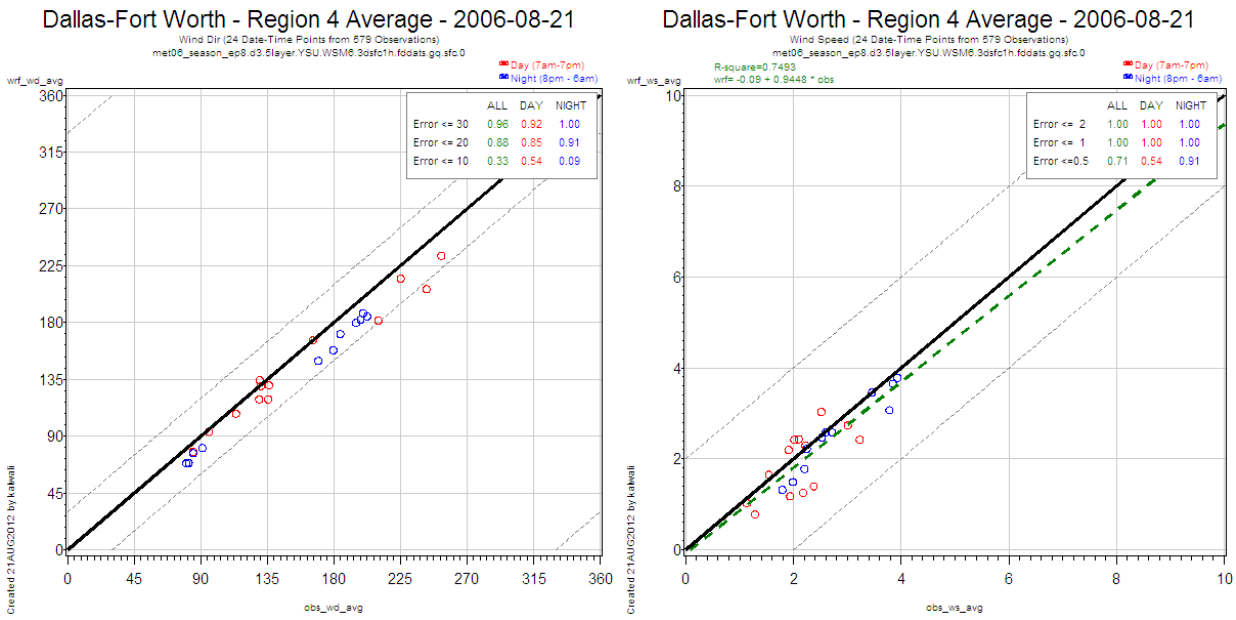

Figure 4-30: August 21, 2006 Wind Direction and Speed Scatter Plots

The light and variable clouds in the immediate vicinity of DFW as shown in Figure 4-31: August 21, 2006 WRFCAMx Cloud Optical Depth and GOES Cloud Fraction was conducive to the production of ozone despite clouds to the west, north, east was replicated by modeling. The Cleburne profiler Figure 4-32: Time-height plot for the Cleburne Profiler on August 21, 2006 that light winds were found to a depth of 2 km from 10 a.m. through the entire afternoon.

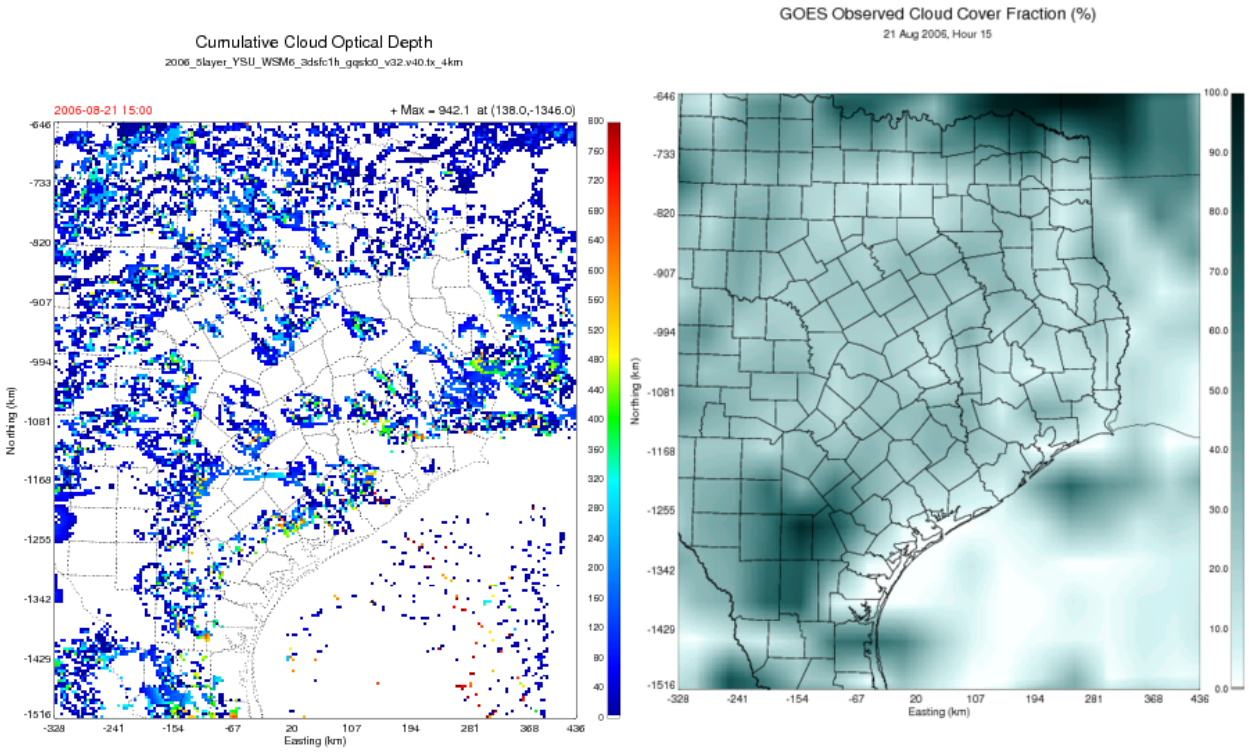

Figure 4-31: August 21, 2006 WRFCAMx Cloud Optical Depth and GOES Cloud Fraction

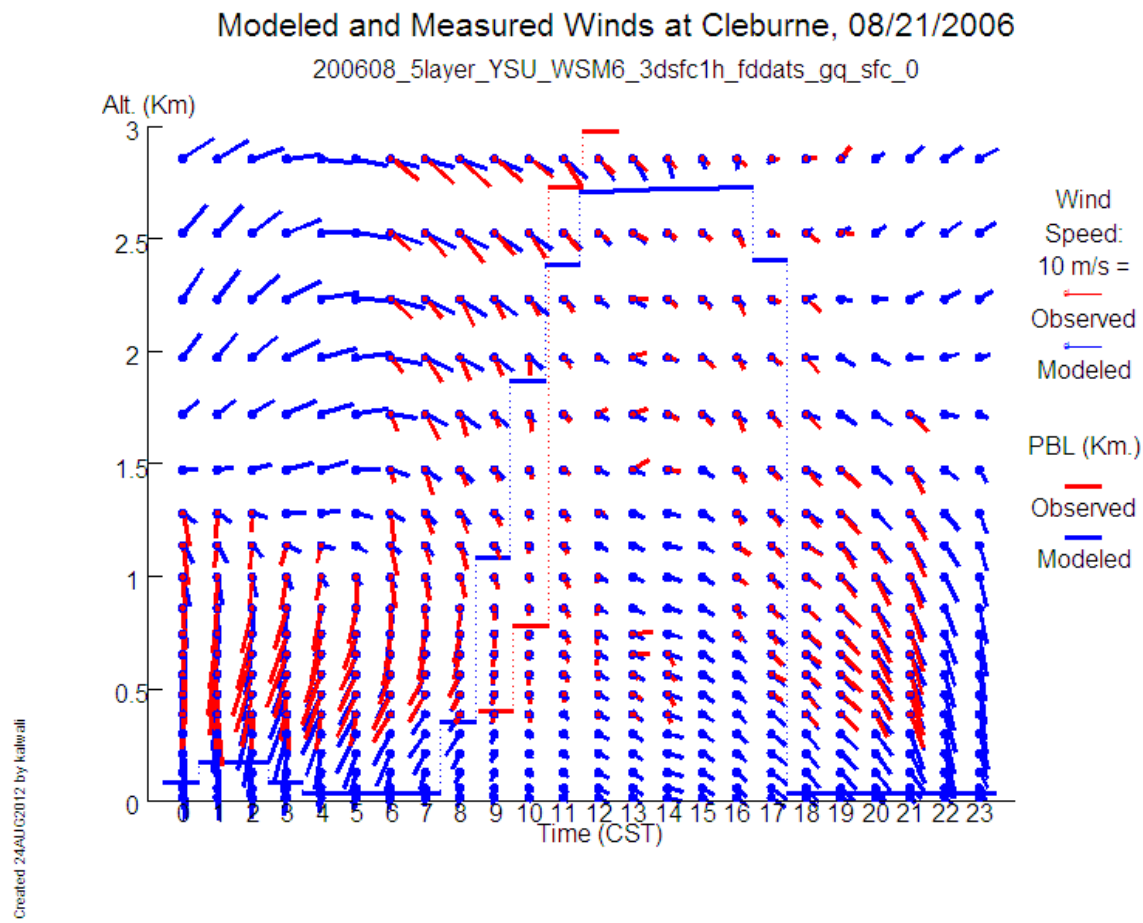

Figure 4-32: Time-height plot for the Cleburne Profiler on August 21, 2006

4.9 August 22, 2006 Performance Evaluation

August 22, 2006 had six monitors with exceedances as opposed to seven from the day before; however, August 22nd reported a slightly higher eight hour average – 91 ppb a Dallas Executive airport rather than the 88 ppb reported at Grapevine. However, the over-prediction by CAMx might be partially attributed to different meteorological modeling performance.

The stationary front identified on August 21st re-established as a cold front on August 22nd. Wind direction errors are now more pronounced as WRF winds have rotated clockwise with respect to observations. Two daytime hours are 180 degrees out of phase Table 4-10: August 22, 2006 Meteorological Modeling Percent Accuracy; Figure 4-33: August 22, 2006 Wind Direction and Speed Scatter Plots.

Table 4-10: August 22, 2006 Meteorological Modeling Percent Accuracy

DFW Area	Wind Direction (°) Error ≤ 30 / 20 / 10	Wind Speed (m/s) Error ≤ 2 / 1 / 0.5	Temperature (°C) Error ≤ 2 / 1 / 0.5
Area Average	58 / 46 / 08	100 / 96 / 79	92 / 42 / 17

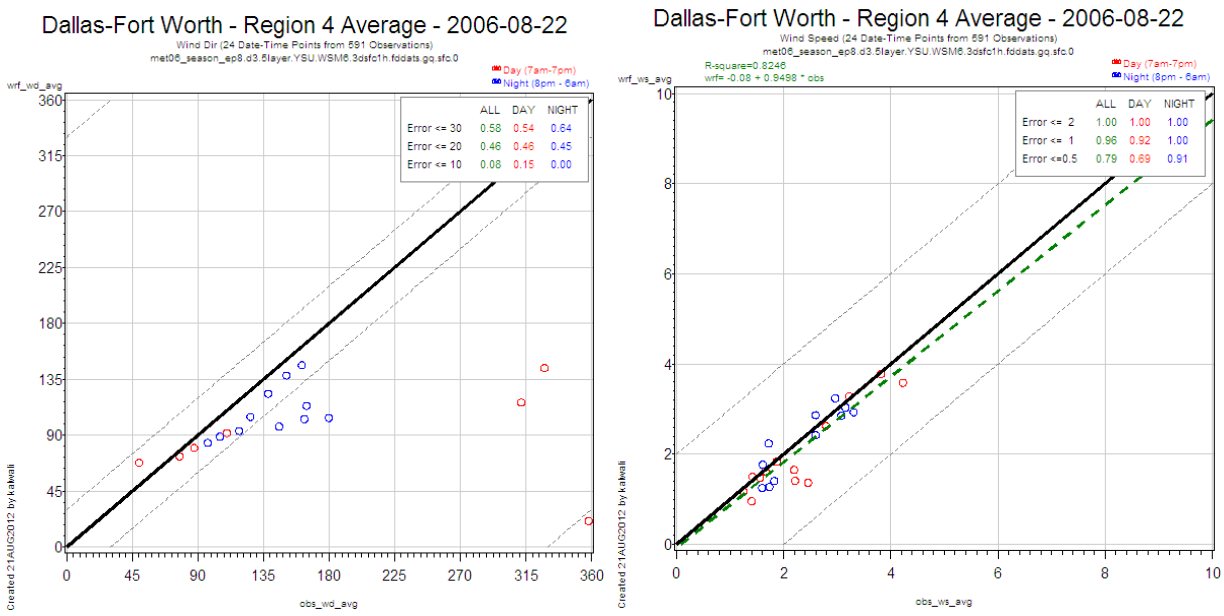

Figure 4-33: August 22, 2006 Wind Direction and Speed Scatter Plots

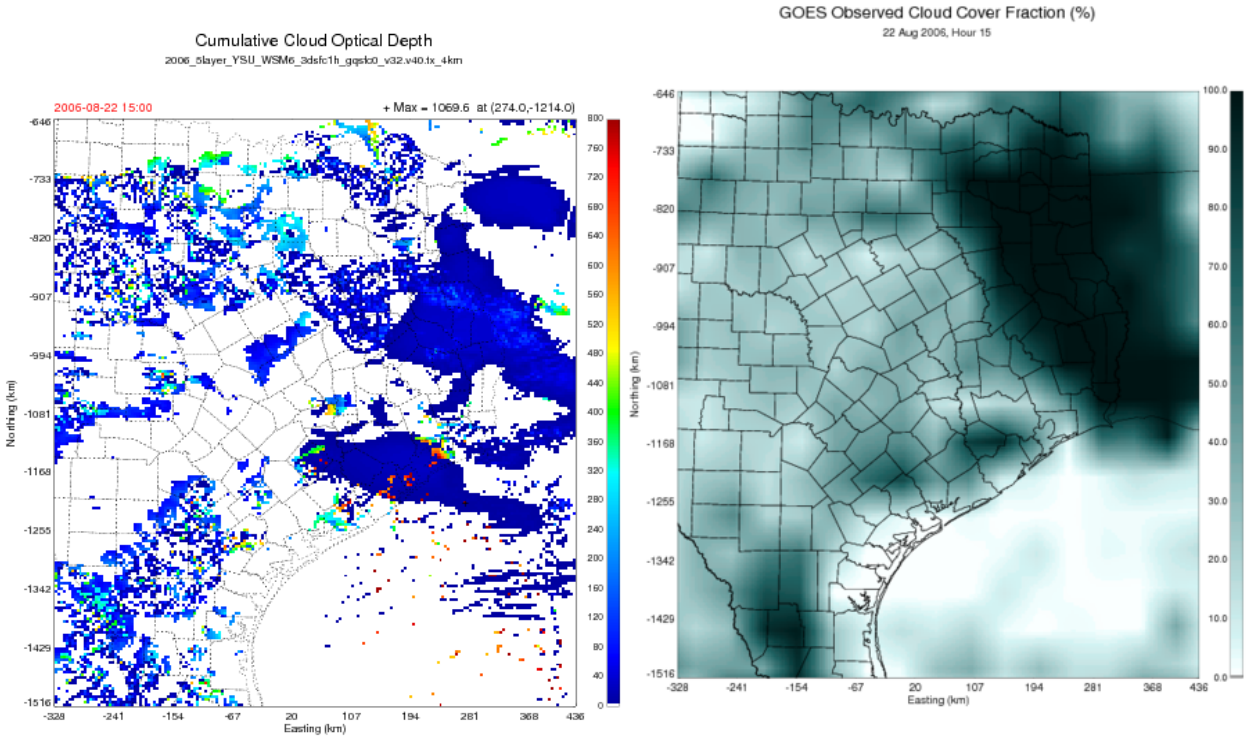

Figure 4-34: August 22, 2006 WRFCAMx Cloud Optical Depth and GOES Cloud Fraction

Although the cloud optical depth calculated from WRF cloud cover is approximately matches the pattern of GOES cloud fraction data Figure 4-34: August 22, 2006 WRFCAMx Cloud Optical Depth and GOES Cloud Fraction the predicted cloud coverage is not as extensive over the DFW area and might have contributed to model over predictions.

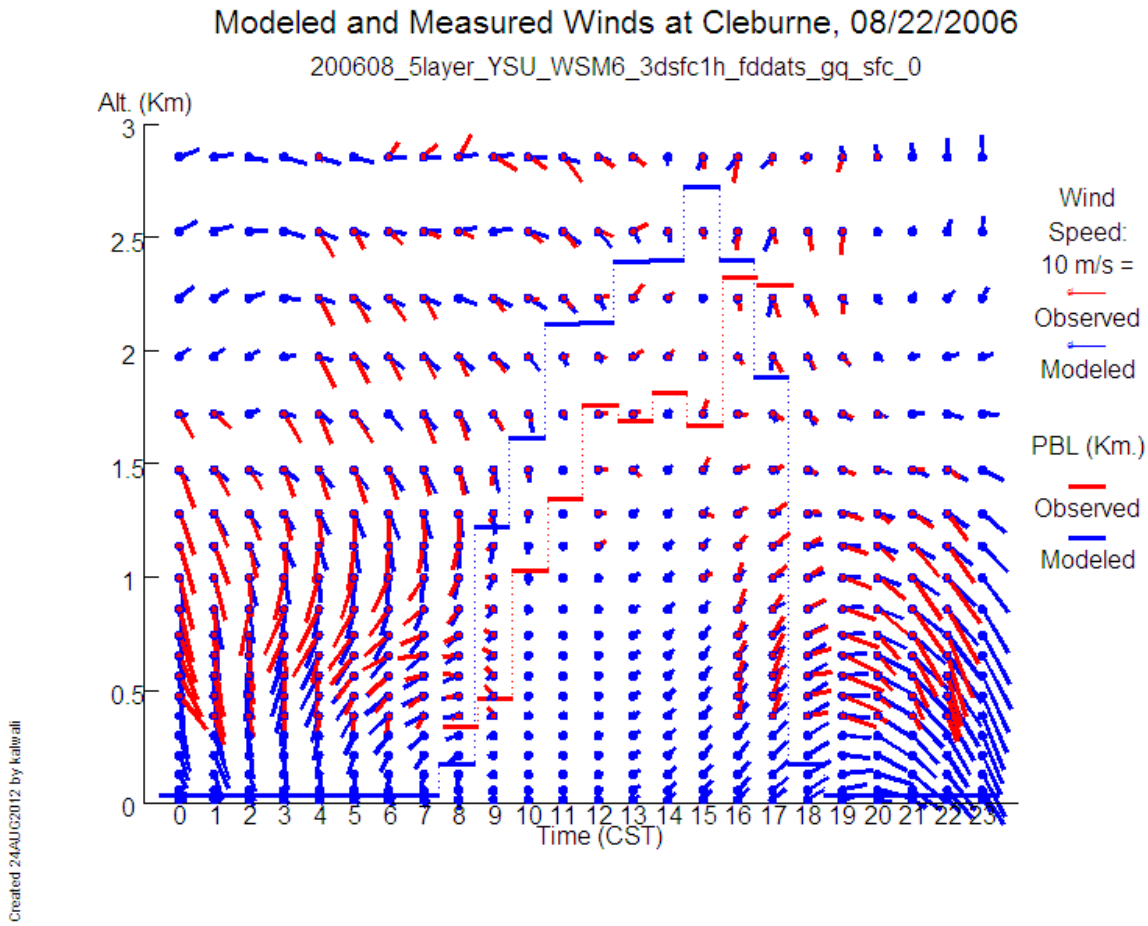

Figure 4-35: Time-height plot for the Cleburne Profiler on August 22, 2006

4.10 September 1, 2006 Performance Evaluation

The high ozone recorded in DFW on August 31 and September 1st followed a front on August 30th.

As seen in Table 4-11: September 1, 2006 Meteorological Modeling Percent Accuracy, WRF wind speed performance was very good, and although the overall pattern of winds on this day was replicated, the wind direction statistics suffered from a bias that migrated from counterclockwise in the morning hours to clockwise over the course of the day as captured in Figure 4-36: September 1, 2006 Wind Direction and Speed Scatter Plots.

Table 4-11: September 1, 2006 Meteorological Modeling Percent Accuracy

DFW Area	Wind Direction (°) Error ≤ 30 / 20 / 10	Wind Speed (m/s) Error ≤ 2 / 1 / 0.5	Temperature (°C) Error ≤ 2 / 1 / 0.5
Area Average	58 / 50 / 25	100 / 88 / 71	88 / 33 / 13

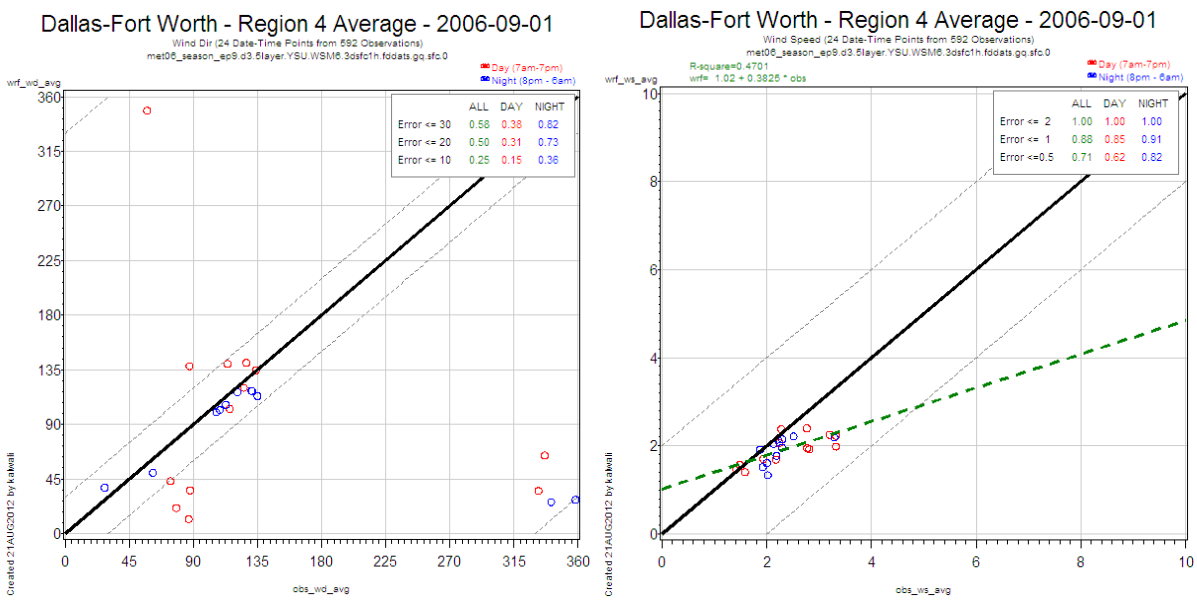

Figure 4-36: September 1, 2006 Wind Direction and Speed Scatter Plots

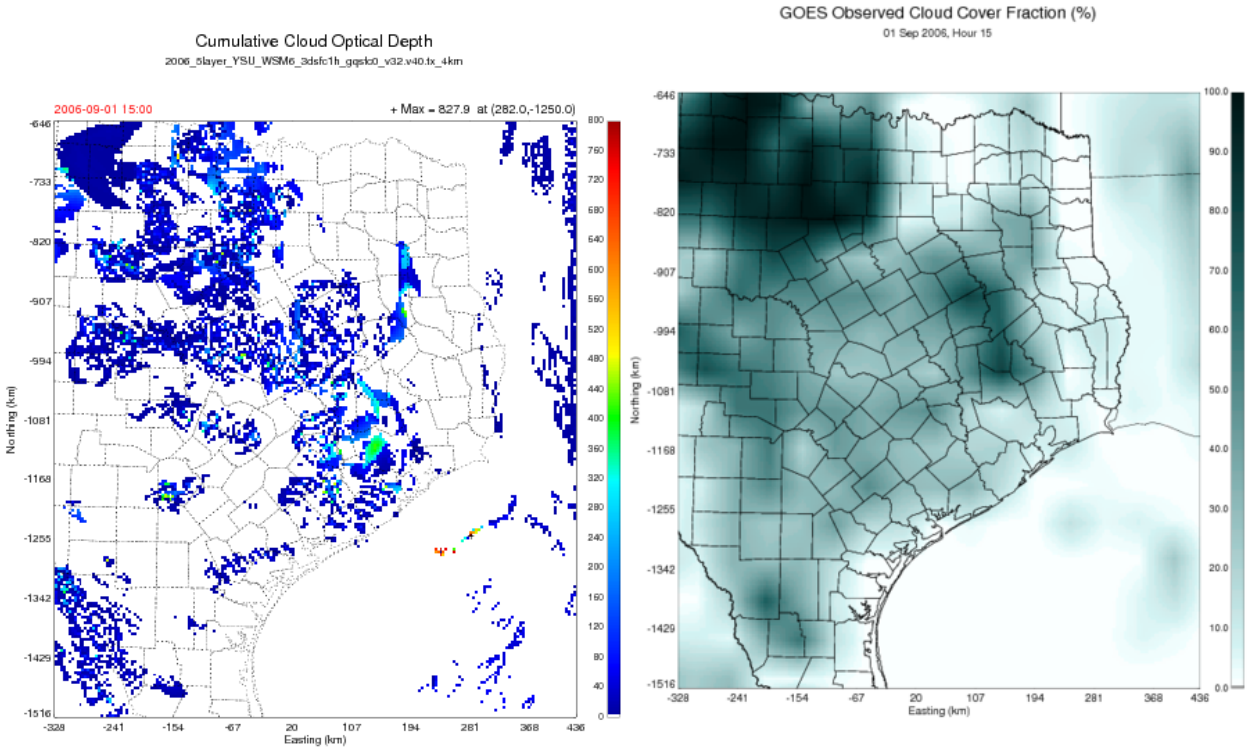

Figure 4-37: September 1, 2006 WRFCAMx Cloud Optical Depth and GOES Cloud Fraction

Unlike the example of June 18, 2006 seen in Figure 4-16 in which WRF predicted clouds, as approximated by the cloud optical depth, hit the DFW are rather than missing it, September 1 predicted cloud optical depth matched the mostly clear skies seen in the GOES data. This may have contributed to the better CAMx model performance seen this day.

Also the wind direction biases seen at the surface monitoring sites in morning and late afternoon (Figure 4-36) are not pronounced during the day between 11 CST and 4 P.M. CST and winds through the PBL seem well characterized as seen in Figure 4-38.

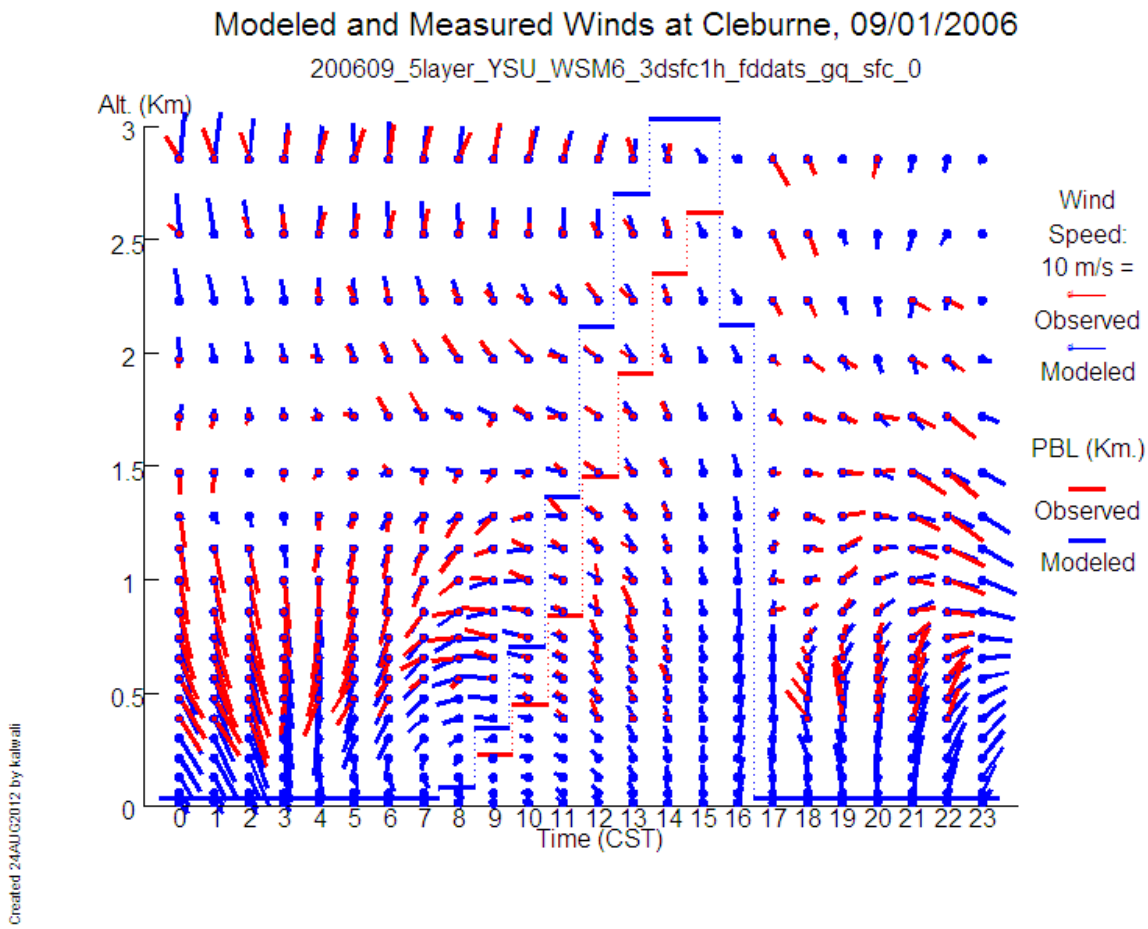

Figure 4-38: Time-height plot for the Cleburne Profiler on September 1, 2006

5. REFERENCES

Banta, R. M., C. J. Senff, J Nielsen-Gammon, L. S. Darby, T. B. Ryerson, R. J. Alvarez, S. P. Sandberg, E. J. Williams and M. Trainer (2005), A bad air day in Houston, *Bulletin of the American Meteorological Society*, *86*(5), 657+, 10.1175/BAMS-86-5-657

Berkowitz, C.M., Spicer, C.W., Doskey, P.V (2005), Hydrocarbon observations and ozone production rates in western Houston during the Texas 2000 air quality study. Atmospheric Environment 39 (19), 3383–3396.

EPA (2007), Guidance on the Use of Models and Other Analyses for Demonstrating Attainment of Air Quality Goals for Ozone, PM2.5, and Regional Haze, http://www.epa.gov/scram001/guidance/guide/final-03-pm-rh-guidance.pdf, EPA-454/B-07-002, 162, Last accessed March 26, 2009.

Grell, G., J. Dudhia, and D. Stauffer (1994), A description of the Fifth Generation Penn State/NCAR Mesoscale Model (MM5), Tech. Rep. NCAR/TN-398+STR, National Center of Atmospheric Research (NCAR) Tech Note.

Janjic, Z. I. (1994), The step-mountain Eta coordinate model: Further developments of the convection, viscous sublayer, and turbulence closure schemes, Mon. Wea. Rev., 122, 927–945.

Knoderer, C. A., S. A. Bratek, C. P. MacDonald (2008), Spatial and Temporal Characteristics of Winds and Mixing During TexAQS-II, Final Report to Texas A&M University for Texas Commission on Environmental Quality Proposal under Grant Activity 582-5-64593-FY08-20, Sonoma Technology Inc, Petaluma, CA, April 2008.

McNider (2009), Stationary Front Experiment Comparison of Flight and Model Data, Final Report for Project H109 to the Houston Advanced Research Center (HARC), http://files.harc.edu/Projects/AirQuality/Projects/H109/H109FinalReport.pdf.

NCEP, (2009), GCIP NCEP Eta model output, CISL RDA: ds609.2 Home Page, http://rda.ucar.edu/datasets/ds609.2/, Last accessed May 13, 2009.

Nielsen-Gammon (2007a), Preliminary Analysis of Ozone Meteorology during TexAQS-II Ozone Episodes, Interim Report to the Texas Commission on Environmental Quality under Proposal for Grant Activity 582-5-64593-FY07-21.

Nielsen-Gammon (2007b), Comprehensive meteorological analysis of TexAQS II episodes, Task 3 Deliverable for Texas Commission on Environmental Quality Proposal for Grant Activity 582-5-64593-FY07-21.

Stauffer, D. R., and N. L. Seaman (1990), Use of four-dimensional data assimilation in a limited area mesoscale model. Part I: Experiments with synoptic-scale data, Mon. Wea. Rev., 118, 1250–1277.

Stauffer, D. R., and N. L. Seaman (1994), Multiscale four-dimensional data assimilation, J. Appl. Meteor., 33, 416–434.

Stauffer, D. R., N. L. Seaman, and F. S. Binkowski (1991), Use of four-dimensional data assimilation in a limited area mesoscale model. Part II: Effects of data assimilation within the planetary boundary layer, Mon. Wea. Rev., 119, 734–754.

TCEQ (2005), 2005 Air Pollution Events, http://www.tceq.texas.gov/airquality/monops/sigevents05.html, Texas Commission on Environmental Quality (TCEQ), Last accessed January 3, 2011.

TCEQ (2006), 2006 Air Pollution Events, http://www.tceq.texas.gov/airquality/monops/sigevents06.html, Texas Commission on Environmental Quality (TCEQ), Last accessed January 3, 2011.

TCEQ (2009), Meteorological modeling performance evaluation products, Texas Commission on Environmental Quality (TCEQ) file transfer protocol (FTP) site, (ftp://ftp.tceq.texas.gov/pub/HGB8H2/mm5).

TCEQ, 2010. Adopted HGB Attainment Demonstration SIP Revision for the 1997 Eight-Hour Ozone Standard (2009-017-SIP-NR), Texas Commission on Environmental Quality, March 2010, http://www.tceq.texas.gov/implementation/air/sip/texas-sip/hgb/hgb-latest-ozone.